Factorization Method for Electromagnetic Inverse Scattering from Biperiodic Structures

Armin Lechleiter* Dinh-Liem Nguyen†

December 23, 2012

Abstract

We investigate the Factorization method as an analytical as well as a numerical tool to solve inverse electromagnetic wave scattering problems from penetrable biperiodic structures in three dimensions. This method constructs a simple criterion whether a given point in space lies inside or outside the penetrable biperiodic structure, yielding a fast imaging algorithm. The required data consists of tangential components of Rayleigh sequences corresponding to (measured) scattered electromagnetic fields. In our setting, the incident electromagnetic fields causing these scattered waves are plane incident electromagnetic waves. We propose on the one hand a rigorous analysis for the Factorization method in this electromagnetic plane wave setting, building upon existing results for the method in the context of inverse electromagnetic scattering from bounded objects and of scalar periodic inverse scattering problems. On the other hand, we provide, to the best of our knowledge, the first three-dimensional numerical examples for electromagnetic inverse scattering from biperiodic structures in three dimensions and consider the dependence of the method on the noise level and on the number of Rayleigh coefficients involved in the imaging process.

1 Introduction

We consider inverse scattering of electromagnetic waves from penetrable biperiodic structures in three dimensions. The biperiodic structures we consider are periodic in the, say, x_1- and x_2-direction, while they are bounded in the x_3-direction. The inverse problem that we treat in this paper is the shape reconstruction of a biperiodic medium from measured data consisting, in principle, of scattered electromagnetic waves, when plane electromagnetic waves are used as incident waves. The problem that we study is motivated by the important applications of such biperiodic structures in, e.g., optics, including diffractive optical filters and organic light-emitting diodes. Non-destructive testing is an important topic to guarantee the proper functioning of such devices.

Inverse scattering from biperiodic structures has been an active field of research in the last years. Uniqueness theorems for determining biperiodic scattering objects from the knowledge of scattered fields can be found in, e.g., [1,8,9,21,36]. (Some of these results only apply to polyhedral

*Center for Industrial Mathematics, University of Bremen, Bibliothekstr. 1, 28359 Bremen, Germany. Email: lechleiter@math.uni-bremen.de

†DEFI, INRIA Saclay–Ile-de-France and Ecole Polytechnique, Route de Saclay, 91128 Palaiseau Cedex, France. Email: dnguyen@cmap.polytechnique.fr

structures.) In the general context of acoustic and electromagnetic inverse scattering, qualitative methods received considerable attention since the Linear Sampling Method was first introduced in [14] for a scalar inverse obstacle scattering problem. This method aims to compute a picture of the shape of the scattering object from measured (near- or far-field) data. Since the method is fast and does not need a-priori knowledge, it has attracted much research during the last 15 years. One can find recent developments concerning the linear sampling method in [10,11]. It is important for the context of this paper to note that the linear sampling method has been extended very recently to inverse scattering involving periodic and biperiodic media in [18, 19, 37]. However, in spite of the advantages of the method, a full mathematical justification still remains open, see [10, 23]. Some results on the justification of (a slight modification of) the linear sampling method have been recently obtained in [3, 6, 23]. The technique applied in these references do, however, not seem to apply to periodic inverse scattering problems since the measurement operators in this context fail to be normal.

As an attempt to improve the theoretical justification of the linear sampling method, the so-called Factorization method has been developed in [22,24]. This method has a rigorous justification, it keeps the previously mentioned advantages of the linear sampling and hence is an interesting tool for shape identification problems in the context of partial differential equations, in particular for inverse scattering problems. However, there is only a restricted class of scattering problems to which the Factorization method can be applied, see [23], due to a crucial assumption of, roughly speaking, positivity (compare Theorem 10 below).

During the last ten years, the Factorization method has been progressively extended to periodic inverse scattering problems: In [4,5] the authors studied the Factorization method for the imaging problem of impenetrable periodic structures with Dirichlet or impedance boundary conditions. The paper [26] considered imaging of penetrable periodic interfaces between two dielectrics in two dimensions. Finally, the thesis [32] considered inverse electromagnetic scattering problems, in a setting that is somewhat different than the one we choose here (see the discussion in the next paragraph).

In the present work we aim to study the Factorization method as a tool for reconstructing the shape of three-dimensional biperiodic structures from data consisting, roughly speaking, of scattered electromagnetic waves. More specifically, the measured data that we consider are the Rayleigh coefficients of evanescent and propagating modes of the scattered fields. These scattered fields are caused by incident electromagnetic plane waves. This setting is different from the one chosen in the thesis [32] where incident conjugated and periodic electromagnetic point sources are used to generate scattering data. These conjugated point sources are unphysical since they do not satisfy the radiation condition, but they are, unfortunately, crucial for the Factorization method with near-field values as measurements. To this end, a special class of plane wave incident fields for scalar inverse periodic scattering problems was first introduced in [4] to avoid the conjugated sources. We extend this plane wave setting in this paper to electromagnetic periodic inverse scattering problems.

Given the tangential components of the Rayleigh coefficients of the scattered fields, the inverse problem we consider is to determine the three-dimensional penetrable biperiodic scatterer. We prove that the Factorization method is able to solve this shape identification problem and that the method provides an efficient tool to image the structure. The numerical behavior of the method for this periodic electromagnetic inverse problem is shown through three-dimensional numerical experiments which are, to the best of our knowledge, the first numerical examples for this method in a biperiodic electromagnetic setting.

The inverse periodic electromagnetic scattering problem we consider is set in full space. This is essentially the reason why we require measurements taken above and below the structure. Indeed, assuming that the biperiodic structure has two distinct top and bottom surfaces, we could only reconstruct the top and bottom surface of the biperiodic structure if we had only access to measurements from above and below, respectively. It is worth to mention that the Factorization method could in a similar way be applied to, e.g., a half-space problem where a penetrable structure is mounted on a perfectly conducting plate. However, treating penetrable structures on top of perfectly conducting biperiodic gratings is a more involved problem that is currently not possible to treat by the Factorization method (for the same reason as for bounded perfectly conducting obstacles – the above-mentioned lack of, roughly speaking, positivity).

To give a brief impression on how the Factorization method works, we need to introduce the real and imaginary parts (aka. the selfadjoint and anti-selfadjoint parts) of a linear operator. If $N : X \to X^*$ is bounded from a reflexive Banach spaces X into the dual space X^* (that is, $(X^*)^*$ is identified with X and the adjoint operator N^* is again bounded from X into X^*), then

$$\operatorname{Re}(N) := \frac{1}{2}(N + N^*), \qquad \operatorname{Im}(N) := \frac{1}{2i}(N - N^*). \tag{1}$$

Later on, N is our notation for the measurement operator of our inverse problem defined on the sequence space $\ell^2(\mathbb{Z}^2)^4$. Additionally, we will introduce certain explicit test sequences $(\hat{\Psi}_{z,j})_{j\in\mathbb{Z}^2}$ depending on the sampling point $z \in \mathbb{R}^3$. The statement of the Factorization method is then, roughly speaking, that the test sequence $(\hat{\Psi}_{z,j})_{j\in\mathbb{Z}^2}$ belongs to the range of the square root of the selfadjoint and non-negative operator

$$N_\sharp := |\operatorname{Re} N| + \operatorname{Im} N$$

if and only if the point $z \in \mathbb{R}^3$ belongs to the support of the biperiodic structure (see Theorem 9 for a detailed formulation with precise assumptions). Since the range of the square root of $N_\sharp$ can be computed using Picard's range criterion, this statement can be easily transformed into a numerical method for imaging the biperiodic structure (see again Theorem 9).

An obvious question arising from this setting of the inverse problem is whether it is feasible in practice. Obtaining precise information about the evanescent modes of a scattered field requires near-field measurements taken close to the surface (one or two wavelengths away from the structure). Due to the recent advantages in near-field optical scanning microscopy [12], such measurements are nowadays available, even if, admittedly, the experimental set-up is far more involved than for far-field measurements. Additionally, some of the incident plane waves we use to excite scattered fields decay exponentially towards the structure. As it is well-known, such fields can be generated using total internal reflection techniques [12], again at the expense of a far more involved experimental set-up compared to propagating incident fields.

Our analysis extends approaches in [4, 23, 25] for scalar periodic inverse scattering problems to Maxwell's equations in a biperiodic setting. We adapt the special two-dimensional plane incident fields introduced in [4] for the periodic scalar case to the three-dimensional electromagnetic problem, which allows us to suitably factorize the near-field operator. Further, a modified version of the method studied in [25] treats the case that the imaginary part of the middle operator in the factorization is just semidefinite. Finally, the necessary properties of the middle operator are obtained, with slight modifications, following the approach in [23] for inverse electromagnetic scattering from bounded inhomogeneous objects.

The numerical examples we show are computed using synthetic scattering data provided by a volume integral equation solver that is presented in detail in the thesis [31]. For scalar problems, the analogous volume integral equation has been investigated in detail in [27,28]. Since the arising linear system is large and dense, and since the evaluation of the integral operator can be computed in order-optimal time (up to logarithmic terms) via the fast Fourier transform, iterative solvers should be used to solve the arising linear system. We used the GMRES algorithm from [20] without restart together with the FFTW3 software package [17] for the fast Fourier transforms to code a forward solver generating the synthetic data we used for the numerical experiments.

The paper is organized as follows: In Section 2 we introduce the direct electromagnetic scattering problem from a biperiodic penetrable structure. Further, we introduce the corresponding inverse problem and the measurement operator that we call, as it is usually done, the near-field operator. Section 3 is dedicated to the study of a factorization of the near-field operator N. In Section 4 we derive analytic properties of the middle operator of the factorization that are crucial to establish the theoretical backbone of the Factorization method. These properties allow to state a characterization of the biperiodic structure in terms of the measured data in Section 5. Finally, Section 6 presents numerical experiments to examine the performance of the method. The appendix contains an abstract range identity theorem that we present without proof. A complete proof of the latter result can be found in the thesis [31, Theorem 3.4.1].

2 Problem Setting

We consider scattering of time-harmonic electromagnetic waves from a biperiodic penetrable structure in $\mathbb{R}^3$. The electric field E and the magnetic field H are governed by the time-harmonic Maxwell equations at frequency $\omega > 0$,

$$\operatorname{curl} H + \mathrm{i}\omega\varepsilon E = \sigma E \qquad \text{in } \mathbb{R}^3, \tag{2}$$

$$\operatorname{curl} E - \mathrm{i}\omega\mu_0 H = 0 \qquad \text{in } \mathbb{R}^3. \tag{3}$$

Here, the electric permittivity ε and the conductivity σ are real bounded and measurable functions which are 2π-periodic in x_1 and x_2, and μ_0 is the constant positive magnetic permeability. Further, we assume that ε equals $\varepsilon_0 > 0$ and that σ vanishes outside the biperiodic structure of finite height. As usual, the problem (2)-(3) has to be completed by a radiation condition that we set up later on using Fourier series. Let us denote the relative material parameter by

$$\varepsilon_{\mathrm{r}} := \frac{\varepsilon + \mathrm{i}\sigma}{\varepsilon_0} \qquad \text{in } \mathbb{R}^3.$$

Note that ε_{r} equals 1 outside the biperiodic structure. Recall that the magnetic permeability μ_0 is constant which motivates us to work with the divergence-free magnetic field, that is, $\operatorname{div} H = 0$ due to (3). Hence, introducing the wave number $k = \omega(\varepsilon_0\mu_0)^{1/2}$ and eliminating the electric field E from (2)-(3), we find that

$$\operatorname{curl}\left(\varepsilon_{\mathrm{r}}^{-1} \operatorname{curl} H\right) - k^2 H = 0 \quad \text{ in } \mathbb{R}^3. \tag{4}$$

Next we define that a function $u : \mathbb{R}^3 \to \mathbb{C}^3$ is called α-quasiperiodic for $\alpha := (\alpha_1, \alpha_2, 0)^\top \in \mathbb{R}^3$ if

$$u(x_1 + 2\pi n_1,\, x_2 + 2\pi n_2, x_3) = e^{2\pi\mathrm{i}\,\alpha\cdot n} u(x_1, x_2, x_3) \quad \text{ for all } n = \begin{pmatrix} n_1 \\ n_2 \\ 0 \end{pmatrix} \in \mathbb{Z}^3$$

and for all $x = (x_1, x_2, x_3)^\top \in \mathbb{R}^3$. Assume that the biperiodic structure is illuminated by α-quasiperiodic incident electric and magnetic fields E^i and H^i, respectively, satisfying

$$\operatorname{curl} H^i + \mathrm{i}\omega\varepsilon_0 E^i = 0, \qquad \operatorname{curl} E^i - \mathrm{i}\omega\mu_0 H^i = 0 \quad \text{in } \mathbb{R}^3.$$

Simple examples for such α-quasiperiodic fields are certain plane waves that we introduce below. Later on, it will be convenient to reformulate (4) in terms of the scattered field H^s, defined by $H^s := H - H^i$. Straightforward computations show that $\operatorname{curl}\operatorname{curl} H^i - k^2 H^i = 0$. Defining the contrast q by

$$q := \varepsilon_{\mathrm{r}}^{-1} - 1,$$

we obtain that

$$\operatorname{curl}\left(\varepsilon_{\mathrm{r}}^{-1}\operatorname{curl} H^s\right) - k^2 H^s = -\operatorname{curl}\left(q \operatorname{curl} H^i\right) \quad \text{in } \mathbb{R}^3. \tag{5}$$

Since ε_{r} is 2π-periodic in x_1 and x_2, and since the right-hand side is α-quasiperiodic, we seek for an α-quasiperiodic solution H^s. Hence, the problem to find the scattered field H^s reduces to one period $(0, 2\pi)^2 \times \mathbb{R}$. We complement this problem by a radiation condition that we set up using (well-known) Fourier techniques. Since the scattered field H^s is α-quasiperiodic, the function $e^{-\mathrm{i}\,\alpha\cdot x} H^s$ is 2π-periodic in x_1 and x_2, and can hence be expanded as a vector-valued Fourier series,

$$e^{-\mathrm{i}\,\alpha\cdot x} H^s(x) = \sum_{n\in\mathbb{Z}^2} \hat{H}_n(x_3) e^{\mathrm{i}(n_1 x_1 + n_2 x_2)}, \quad x = (x_1, x_2, x_3)^\top \in \mathbb{R}^3. \tag{6}$$

The Fourier coefficients $\hat{H}_n(x_3) \in \mathbb{C}^3$ for $n \in \mathbb{Z}^2$ are defined by

$$\hat{H}_n(x_3) = \frac{1}{4\pi^2} \int_0^{2\pi} \int_0^{2\pi} H^s(x_1, x_2, x_3) e^{-\mathrm{i}\,\alpha_n\cdot x}\,\mathrm{d}x_1\,\mathrm{d}x_2\,, \tag{7}$$

where

$$\alpha_n := (\alpha_{1,n}, \alpha_{2,n}, 0)^\top := (\alpha_1 + n_1, \alpha_2 + n_2, 0)^\top \in \mathbb{R}^3.$$

We define, for $n \in \mathbb{Z}^2$,

$$\beta_n := \begin{cases} \sqrt{k^2 - |\alpha_n|^2}, & k^2 \geq |\alpha_n|^2, \\ \mathrm{i}\sqrt{|\alpha_n|^2 - k^2}, & k^2 < |\alpha_n|^2. \end{cases}$$

For a technical reason we assume in the following that k is not a Wood's anomaly (or, equivalently, that the frequency ω is not a Rayleigh frequency), i.e.,

$$\beta_n \neq 0 \quad \text{for all } n \in \mathbb{Z}^2. \tag{8}$$

The technical reason behind this assumption is basically that the representation of a certain Green's tensor that we introduce in Section 5 (see (31)) is not well-defined at a Wood's anomaly.

Recall that $\varepsilon_{\mathrm{r}}^{-1}$ equals one outside the structure. This means that $\varepsilon_{\mathrm{r}}^{-1} = 1$ and $q = 0$ for $|x_3| > h$ where $h > \sup\{|x_3| : (x_1, x_2, x_3)^\top \in \operatorname{supp}(q)\}$. Thus, it holds that $\operatorname{div} H^s$ vanishes for $|x_3| > h$, and equation (5) becomes $(\Delta + k^2) H^s = 0$ in $\{|x_3| > h\}$. Using separation of variables and choosing the outwards propagating solution, we set up a radiation condition in form of a Rayleigh expansion condition, prescribing that H^s can be written as

$$H^s(x) = \sum_{n\in\mathbb{Z}^2} \hat{H}_n^{\pm} e^{\mathrm{i}(\alpha_n\cdot x + \beta_n |x_3 - h|)} \quad \text{for } x_3 \gtrless \pm h, \tag{9}$$

where $(\hat{H}_n^{\pm})_{n\in\mathbb{Z}^2}$ are the Rayleigh sequences given by

$$\hat{H}_n^{\pm} := \hat{H}_n(\pm h) = \frac{1}{4\pi^2}\int_0^{2\pi}\int_0^{2\pi} H^s(x_1, x_2, \pm h)e^{-\mathrm{i}\,\alpha_n\cdot x}\,\mathrm{d}x_1\,\mathrm{d}x_2\,, \quad n\in\mathbb{Z}^2.$$

In the following, a function which satisfies (9) is called radiating. Note that only a finite number of terms in (9) are propagating plane waves, also called propagating modes, and that the remaining terms are evanescent modes that are exponentially decaying. This implies that the series in (9) converges uniformly on compact subsets of $\{|x_3| > h\}$ whenever the scattered field H^s restricted to $\Gamma_{\pm h} := (0, 2\pi)^2 \times \{\pm h\}$ belongs to, e.g., $H^s(\Gamma_{\pm h})^3$ for some $s \in \mathbb{R}$. (The latter condition will always be satisfied since we will seek for divergence-free $H(\mathrm{curl})$-solutions to the scattering problem.)

Denote by $D \subset \Omega$ an open set such that $\overline{D}$ is the support of the contrast q in one period $\Omega := (0, 2\pi)^2 \times \mathbb{R}$, that is,

$$\mathrm{supp}(q) = \overline{D} \subset \overline{\Omega}.$$

We state an assumption that is necessary for the subsequent factorization method.

Assumption 1. *We assume that $D \subset \Omega$ is a Lipschitz domain and that there exists $c > 0$ such that $\mathrm{Re}\,(q) \geq c > 0$ and $\mathrm{Im}\,(q) \leq 0$ almost everywhere in D. We assume further that $\Omega \setminus D$ consists of at most two connected components and that each connected component of $\Omega \setminus D$ is unbounded.*

Remark 2. *One can replace the assumption that $\mathrm{Re}\,(q) \geq c > 0$ by the assumption that $\mathrm{Re}\,(q) \leq -c < 0$. However, if $\mathrm{Re}\,(q)$ changes sign, then it is currently not known how to prove the fundamental characterization result of method (see Theorem 9 below). Nevertheless, the factorization of the measurement operator that we show in the next section holds independently of the sign of $\mathrm{Re}\,(q)$. The second part of Assumption 1 states that, roughly speaking, D has no holes.*

Considering a more general source term on the right hand side of (5), we obtain the following direct problem: Given $f \in L^2(D)^3$, find a radiating solution $u : \Omega \to \mathbb{C}^3$ in a suitable function space to

$$\mathrm{curl}\left(\varepsilon_{\mathrm{r}}^{-1}\,\mathrm{curl}\,u\right) - k^2 u = -\,\mathrm{curl}\left(q/\sqrt{|q|}\,f\right) \qquad \text{in } \Omega. \tag{10}$$

Obviously, if u is a solution of (5) then u solves (10) for the right-hand side $f = \sqrt{|q|}\,\mathrm{curl}\,H^i$.

For a variational formulation of the problem (10), we define

$$\begin{aligned}
H(\mathrm{curl}, \mathcal{O}) &= \left\{v \in L^2(\mathcal{O})^3 : \mathrm{curl}\,v \in L^2(\mathcal{O})^3\right\} \quad \text{for any Lipschitz domain } \mathcal{O},\\
H_{\mathrm{loc}}(\mathrm{curl}, \mathbb{R}^3) &= \left\{v : \mathbb{R}^3 \to \mathbb{C}^3 : v|_B \in H(\mathrm{curl}, B) \text{ for all balls } B \subset \mathbb{R}^3\right\},\\
H_{\alpha,\mathrm{loc}}(\mathrm{curl}, \Omega) &= \left\{u \in H_{\mathrm{loc}}(\mathrm{curl}, \Omega) : u = U|_\Omega \text{ for some } \alpha\text{-quasiperiodic } U \in H_{\mathrm{loc}}(\mathrm{curl}, \mathbb{R}^3)\right\},
\end{aligned}$$

and

$$\Omega_h = (0, 2\pi)^2 \times (-h, h) \qquad \text{for } h > \sup\{|x_3| : (x_1, x_2, x_3)^\top \in \overline{D}\},$$

with boundaries $\Gamma_{\pm h} = (0, 2\pi)^2 \times \{\pm h\}$. The variational formulation to the problem (10) is to find a radiating solution $u \in H_{\alpha,\mathrm{loc}}(\mathrm{curl}, \Omega)$ such that

$$\int_\Omega (\varepsilon_{\mathrm{r}}^{-1}\,\mathrm{curl}\,u \cdot \mathrm{curl}\,\overline{\psi} - k^2 u \cdot \overline{\psi})\,\mathrm{d}x = -\int_\Omega q/\sqrt{|q|} f \cdot \mathrm{curl}\,\overline{\psi}\,\mathrm{d}x \tag{11}$$

for all $\psi \in H_{\alpha,\mathrm{loc}}(\mathrm{curl},\Omega)$ with compact support. Existence and uniqueness of this problem can be obtained for all but possibly a discrete set of exceptional positive wave numbers, see e.g. [7,15,34]; the set of exceptional wave numbers moreover does not possess a finite accumulation point.

In the sequel we *assume* that the wave number $k > 0$ is chosen such that (11) is uniquely solvable for all $f \in L^2(D)^3$. Then we can define a linear and bounded solution operator G mapping the source f to the Rayleigh sequences of the first two components of $u \in H_{\alpha,\mathrm{loc}}(\mathrm{curl},\Omega)$, solution to (11),

$$G : L^2(D)^3 \to \ell^2(\mathbb{Z}^2)^4, \quad f \mapsto (\hat{u}^+_{1,j}, \hat{u}^-_{1,j}, \hat{u}^+_{2,j}, \hat{u}^-_{2,j})_{j\in\mathbb{Z}^2} \in \ell^2(\mathbb{Z}^2)^4. \tag{12}$$

The Rayleigh sequences $\left(\hat{u}^+_{(1,2),j}\right)_{j\in\mathbb{Z}^2}$ of the first two components $u_{1,2}$ of $u = (u_1,u_2,u_3)^\top$ above the biperiodic electromagnetic structure are explicitly given by

$$\hat{u}^+_{(1,2),j} = \frac{1}{4\pi^2}\int_{\Gamma_h} u_{1,2}(x)\, e^{-\mathrm{i}\,\alpha_j\cdot x}\,\mathrm{d}S = \frac{1}{4\pi^2}\int_0^{2\pi}\int_0^{2\pi} u_{1,2}(x_1,x_2,h)e^{-\mathrm{i}\,\alpha_j\cdot x}\,\mathrm{d}(x_1,x_2)\,. \tag{13}$$

Analogously, the Rayleigh sequences $\left(\hat{u}^-_{(1,2),j}\right)_{j\in\mathbb{Z}^2}$ can be computed by replacing h by $-h$ in the last aligned equation. Note that the boundedness of the solution operator G follows from the boundedness of $f \mapsto u$ from $L^2(D)^3$ into $H(\mathrm{curl},\Omega_h)$, from the fact that $\operatorname{div} u = 0$ which yields that $u \in H^1(\Omega_h)$ due to [33], and finally from the trace theorem in $H^1(\Omega_h)$ which shows that the Rayleigh coefficients $(\hat{u}^\pm_{(1,2),j})_{j\in\mathbb{Z}^2} \in \ell^2$ are bounded in terms of $\|u\|_{H^1(\Omega_h)}$.

Now we introduce the notation

$$\tilde{b} = \begin{pmatrix} b_1 \\ b_2 \\ -b_3 \end{pmatrix} \quad \text{for any vector } b = \begin{pmatrix} b_1 \\ b_2 \\ b_3 \end{pmatrix} \in \mathbb{C}^3.$$

To obtain the data for the Factorization method we consider the following α-quasiperiodic plane waves

$$\varphi^{(l)\pm}_j = p^{(l)}_j e^{\mathrm{i}(\alpha_j\cdot x+\beta_j x_3)} \pm \tilde{p}^{(l)}_j e^{\mathrm{i}(\alpha_j\cdot x-\beta_j x_3)}, \quad l = 1,2, \quad j \in \mathbb{Z}^2, \tag{14}$$

where the polarizations $p^{(1,2)}_j \in \mathbb{C}^3 \setminus \{0\}$ are defined as

$$p^{(1)}_j = \frac{1}{(|\beta_j|^2+\alpha^2_{2,j})^{1/2}}\begin{pmatrix} 0 \\ \beta_j \\ -\alpha_{2,j} \end{pmatrix}, \quad p^{(2)}_j = \frac{1}{(|\beta_j|^2+\alpha^2_{1,j})^{1/2}}\begin{pmatrix} -\beta_j \\ 0 \\ \alpha_{1,j} \end{pmatrix}, \quad j \in \mathbb{Z}^2.$$

Since $\alpha_j = (\alpha_{1,j},\alpha_{2,j},0)^\top \in \mathbb{R}^3$ is real-valued, this choice implies that

$$|p^{(1)}_j| = |p^{(2)}_j| = 1 \quad \text{and} \quad p^{(1)}_j \times p^{(2)}_j = \frac{\beta_j}{(|\beta_j|^2+\alpha^2_{2,j})^{1/2}(|\beta_j|^2+\alpha^2_{1,j})^{1/2}}\begin{pmatrix} \alpha_{1,j} \\ \alpha_{2,j} \\ \beta_j \end{pmatrix} \quad \text{for } j \in \mathbb{Z}^2. \tag{15}$$

Due to Assumption 8 ($\beta_j \neq 0$ for all $j \in \mathbb{Z}^2$), the polarizations $p^{(1)}_j$ and $p^{(2)}_j$ are hence linearly independent. Additionally, the vector waves $\varphi^{(l)\pm}_j$ are divergence-free functions, because

$$p^{(1)}_j \cdot \begin{pmatrix} \alpha_{1,j} \\ \alpha_{2,j} \\ \beta_j \end{pmatrix} = p^{(2)}_j \cdot \begin{pmatrix} \alpha_{1,j} \\ \alpha_{2,j} \\ \beta_j \end{pmatrix} = 0 \qquad \text{for all } j \in \mathbb{Z}^2. \tag{16}$$

Remark 3. *For all subsequent statements it would be sufficient to choose linear independent polarizations of unit length in* $\mathbb{C}^3$ *such that*(16) *holds. Despite our above explicit choice of the polarizations, we nevertheless work in the rest of the paper with the (implicit) notation* $p_j^{(1)} = (p_{1,j}^{(1)}, p_{2,j}^{(1)}, p_{3,j}^{(1)})^\top$*, to ensure that all possible choices are still included in our analysis. (The same index notation as for* $p_j^{(1)}$ *is used for* $p_j^{(2)}$*.)*

Due to the linearity of the partial differential equation (11), any linear combination of incident fields will lead to a corresponding linear combination of the resulting scattered fields. We obtain such linear combination using sequences

$$(a_j)_{j\in\mathbb{Z}^2} = \left(a_j^{(1)+}, a_j^{(1)-}, a_j^{(2)+}, a_j^{(2)-}\right)^\top_{j\in\mathbb{Z}^2} \in \ell^2(\mathbb{Z}^2)^4$$

and define the corresponding superposition operator $H : \ell^2(\mathbb{Z}^2)^4 \to L^2(D)^3$ by

$$H(a_j) = \sqrt{|q|} \sum_{j\in\mathbb{Z}^2} \frac{1}{\beta_j w_j} \left[a_j^{(1)+} \operatorname{curl} \varphi_j^{(1)+} + a_j^{(2)+} \operatorname{curl} \varphi_j^{(2)+} + a_j^{(1)-} \operatorname{curl} \varphi_j^{(1)-} + a_j^{(2)-} \operatorname{curl} \varphi_j^{(2)-}\right], \quad (17)$$

where the role of the coefficients

$$w_j := \begin{cases} \mathrm{i}, & k^2 > \alpha_j^2, \\ \exp(-\mathrm{i}\beta_j h), & k^2 < \alpha_j^2, \end{cases}$$

is essentially to reduce technical difficulties in some of the later computations. The boundedness of H will be shown in the beginning of the next Section 3.

Given a sequence $(a_j) \in \ell^2(\mathbb{Z}^2)^4$ we can build incident electromagnetic waves of the form $H(a_j)$ (see 17) and measure the tangential component of the electromagnetic wave that is scattered from the periodic inhomogeneous medium. Equivalently, we can record the tangential components of the Rayleigh sequences (see (13)) of the scattered wave. The linear operator mapping $(a_j) \in \ell^2(\mathbb{Z}^2)^4$ to the Rayleigh sequences of the scattered electromagnetic field is the so-called near-field operator

$$N : \ell^2(\mathbb{Z}^2)^4 \to \ell^2(\mathbb{Z}^2)^4, \qquad [N(a_j)]_n := \left(\hat{u}_{1,n}^+, \hat{u}_{1,n}^-, \hat{u}_{2,n}^+, \hat{u}_{2,n}^-\right)^\top, \quad n \in \mathbb{Z}^2,$$

where $u \in H_{\alpha,\mathrm{loc}}(\operatorname{curl}, \Omega)$ is the radiating solution to (11) for the source $f = H(a_j)$. From the definition of the solution operator G it is now clear that (at least formally, since H has not yet been proven to be bounded)

$$N = GH \qquad \text{in } \ell^2(\mathbb{Z}^2)^4. \quad (18)$$

The inverse scattering problem that we investigate in the rest of this paper is to reconstruct the support $\overline{D}$ of the contrast $q = \varepsilon_{\mathrm{r}}^{-1} - 1$ of the periodic inhomogeneous medium when the near-field operator N is given as data. Note that this data is equivalent to know all Rayleigh coefficients of the scattered fields corresponding to all incident fields $\varphi_j^{(l)\pm}$ from (14). Since all evanescent terms in the Rayleigh expansion (9) decay exponentially away from the biperiodic structure, it is clear that reliable measurements of the Rayleigh coefficients can only be achieved close (in terms of the wavelength) to the structure. Note, moreover, that rigorous mathematical identification results for the general class of structures that we consider here require the knowledge of all Rayleigh coefficients, see, e.g., [21].

3 Factorization of the Near-Field Operator

We study the inverse problem of reconstructing the support of a penetrable biperiodic structure from near-field measurements using the Factorization method. One of the important steps of this method that is to find a suitable factorization of the near-field operator N. This factorization is, basically, the content of this section. Before we state the factorization of the near-field operator, we show in the next lemma crucial properties of $H : \ell^2(\mathbb{Z}^2)^4 \to L^2(D)^3$ and its $L^2(D)^3$-adjoint H^*. To this end, it is convenient to introduce the sequence $(w_j^*)_{j\in\mathbb{Z}^2}$, defined by

$$w_j^* := \begin{cases} \exp(-\mathrm{i}\beta_j h), & k^2 > \alpha_j^2, \\ \mathrm{i}, & k^2 < \alpha_j^2, \end{cases} \qquad j \in \mathbb{Z}^2.$$

Lemma 4. *For $p_j^{(l)} = (p_{1,j}^{(l)}, p_{2,j}^{(l)}, p_{3,j}^{(l)})^\top$, $j \in \mathbb{Z}^2$, $l = 1, 2$, defined in (15), the operator $H : \ell^2(\mathbb{Z}^2)^4 \to L^2(D)^3$ is compact and injective, and its adjoint $H^* : L^2(D)^3 \to \ell^2(\mathbb{Z}^2)^4$ satisfies*

$$(H^* f)_j = 8\pi^2 w_j^* \begin{pmatrix} \overline{p_{1,j}^{(1)}}(\hat{u}_{1,j}^+ + \hat{u}_{1,j}^-) + \overline{p_{2,j}^{(1)}}(\hat{u}_{2,j}^+ + \hat{u}_{2,j}^-) \\ \overline{p_{1,j}^{(2)}}(\hat{u}_{1,j}^+ + \hat{u}_{1,j}^-) + \overline{p_{2,j}^{(2)}}(\hat{u}_{2,j}^+ + \hat{u}_{2,j}^-) \\ \overline{p_{1,j}^{(1)}}(\hat{u}_{1,j}^+ - \hat{u}_{1,j}^-) + \overline{p_{2,j}^{(1)}}(\hat{u}_{2,j}^+ - \hat{u}_{2,j}^-) \\ \overline{p_{1,j}^{(2)}}(\hat{u}_{1,j}^+ - \hat{u}_{1,j}^-) + \overline{p_{2,j}^{(2)}}(\hat{u}_{2,j}^+ - \hat{u}_{2,j}^-) \end{pmatrix}, \quad j \in \mathbb{Z}^2, \tag{19}$$

where $(\hat{u}_{1,j}^+, \hat{u}_{1,j}^-, \hat{u}_{2,j}^+, \hat{u}_{2,j}^-)_{j\in\mathbb{Z}^2}^\top$ are the Rayleigh sequences of the first two components of the radiating variational solution $u \in H_{\alpha,loc}(\mathrm{curl}, \Omega)$ to $\mathrm{curl}^2 u - k^2 u = \mathrm{curl}(\sqrt{|q|} f)$ in Ω.

Proof. We first compute the formal adjoint of H and show afterwards that the formal adjoint defines a bounded operator,

$$\begin{aligned} \int_D H(a_j)\overline{f}\,\mathrm{d}x &= \sum_{j\in\mathbb{Z}^2} \left[\sum_{l=1,2} \frac{a_j^{(l)+}}{\beta_j w_j} \int_D \sqrt{|q|}\overline{f} \cdot \mathrm{curl}\, \varphi_j^{(l)+}\,\mathrm{d}x + \sum_{l=1,2} \frac{a_j^{(l)-}}{\beta_j w_j} \int_D \sqrt{|q|}\overline{f} \cdot \mathrm{curl}\, \varphi_j^{(l)-}\,\mathrm{d}x \right] \\ &= \left\langle (a_j), \left(\int_D \sqrt{|q|} f \cdot \overline{\left(\frac{\mathrm{curl}\, \varphi_j^{(l)+}}{\beta_j w_j} \right)}\,\mathrm{d}x, \int_D \sqrt{|q|} f \cdot \overline{\left(\frac{\mathrm{curl}\, \varphi_j^{(l)-}}{\beta_j w_j} \right)}\,\mathrm{d}x \right)_{l=1,2} \right\rangle_{\ell^2(\mathbb{Z}^2)^4}. \end{aligned}$$

Note that the equation $\mathrm{curl}^2 u - k^2 u = \mathrm{curl}(\sqrt{|q|} f)$ in Ω with Rayleigh expansion condition is uniquely solvable for all wave number $k > 0$. The Fredholm property can be obtained as in [7,15,34], and using integral representation formulas from Theorem 3.1 in [32] one shows the uniqueness. Now we define $v_j^{(l)\pm} = \varphi_j^{(l)\pm}/(\beta_j w_j)$ and consider a smooth function $\phi \in C^\infty(\mathbb{R})$ such that $\phi = 1$ in $(-h, h)$, $\phi = 0$ in $\mathbb{R} \setminus \overline{(-2h, 2h)}$. Then $\phi v_j^{(l)\pm}$ belongs to $H_\alpha(\mathrm{curl}, \Omega)$ and has compact support in $\{|x_3| \le 2h\}$. Assume that $u \in H_{\alpha,\mathrm{loc}}(\mathrm{curl}, \Omega)$ is the variational radiating solution to $\mathrm{curl}^2 u - k^2 u = -\mathrm{curl}(\sqrt{|q|} f)$ in Ω. Then

$$\begin{aligned} \int_D \sqrt{|q|} f \cdot \mathrm{curl}\, \overline{v_j^{(l)\pm}}\,\mathrm{d}x &= \int_{\Omega_h} \left(\mathrm{curl}\, u \cdot \mathrm{curl}\, \overline{v_j^{(l)\pm}} - k^2 u \cdot \overline{v_j^{(l)\pm}} \right) \mathrm{d}x \\ &\quad + \int_{\Omega_{2h}\setminus\Omega_h} \left(\mathrm{curl}\, u \cdot \mathrm{curl}(\overline{\phi v_j^{(l)\pm}}) - k^2 u \cdot \overline{\phi v_j^{(l)\pm}} \right) \mathrm{d}x\,. \end{aligned}$$

Now using Green's theorems and exploiting the fact that $v_j^{(l)\pm}$ and u are divergence-free solutions to the Helmholtz equation in $\mathbb{R}^3$ and $\Omega \setminus \Omega_h$, respectively, we obtain that

$$\begin{aligned}\int_D \sqrt{|q|} f \cdot \operatorname{curl} \overline{v_j^{(l)\pm}} \,\mathrm{d}x =& \int_{\Gamma_h} \left(e_3 \times \operatorname{curl} u \cdot \overline{v_j^{(l)\pm}} - e_3 \times \operatorname{curl} \overline{v_j^{(l)\pm}} \cdot u \right) \mathrm{d}S \\ &+ \int_{\Gamma_{-h}} \left(e_3 \times \operatorname{curl} \overline{v_j^{(l)\pm}} \cdot u - e_3 \times \operatorname{curl} u \cdot \overline{v_j^{(l)\pm}} \right) \mathrm{d}S \\ =& \left(\int_{\Gamma_h} - \int_{\Gamma_{-h}} \right) \left[\partial_3 \overline{v_{2,j}^{(l)\pm}} u_2 - \partial_3 u_2 \overline{v_{2,j}^{(l)\pm}} + \partial_3 \overline{v_{1,j}^{(l)\pm}} u_1 - \partial_3 u_1 \overline{v_{1,j}^{(l)\pm}} \right] \mathrm{d}S \,.\end{aligned} \tag{20}$$

Note that

$$\overline{v_{1,j}^{(l)+}} = \overline{\begin{pmatrix} p_{1,j}^{(l)} \\ \beta_j w_j \end{pmatrix}} (e^{\mathrm{i}\beta_j x_3} + e^{-\mathrm{i}\beta_j x_3}) e^{-\mathrm{i}\alpha_j \cdot x} \quad \text{and} \quad \partial_3 \overline{v_{1,j}^{(l)+}} = \mathrm{i}\beta_j \overline{\begin{pmatrix} p_{1,j}^{(l)} \\ \beta_j w_j \end{pmatrix}} (e^{\mathrm{i}\beta_j x_3} - e^{-\mathrm{i}\beta_j x_3}) e^{-\mathrm{i}\alpha_j \cdot x}.$$

Thus, we obtain by straightforward computations that

$$\int_{\Gamma_h} \left(\partial_3 \overline{v_{1,j}^{(l)+}} u_1 - \partial_3 u_1 \overline{v_{1,j}^{(l)+}} \right) \mathrm{d}S = \sum_{n \in \mathbb{Z}^2} \hat{u}_{1,n}^+ \int_{\Gamma_h} e^{\mathrm{i}\alpha_n \cdot x} \left[\partial_3 \overline{v_{1,j}^{(l)+}} - i\beta_n \overline{v_{1,j}^{(l)+}} \right] \mathrm{d}S = 8\pi^2 w_j^* \overline{p_{1,j}^{(l)}} \hat{u}_{1,j}^+.$$

Similarly, we also have

$$\begin{aligned}\int_{\Gamma_h} \left(\partial_3 \overline{v_{2,j}^{(l)+}} u_2 - \partial_3 u_2 \overline{v_{2,j}^{(l)+}} \right) \mathrm{d}S &= 8\pi^2 w_j^* \overline{p_{2,j}^{(l)}} \hat{u}_{2,j}^+, \\ \int_{\Gamma_{-h}} \left(\partial_3 \overline{v_{2,j}^{(l)+}} u_2 - \partial_3 u_2 \overline{v_{2,j}^{(l)+}} + \partial_3 \overline{v_{1,j}^{(l)+}} u_1 - \partial_3 u_1 \overline{v_{1,j}^{(l)+}} \right) \mathrm{d}S &= -8\pi^2 w_j^* \left(\overline{p_{1,j}^{(l)}} \hat{u}_{1,j}^- + \overline{p_{2,j}^{(l)}} \hat{u}_{2,j}^- \right).\end{aligned}$$

Now substituting the last two equations into (20) we derive first that

$$\int_D \sqrt{|q|} f \cdot \operatorname{curl} \overline{v_j^{(l)+}} \,\mathrm{d}x = 8\pi^2 w_j^* \left(\overline{p_{1,j}^{(l)}} \hat{u}_{1,j}^- + \overline{p_{2,j}^{(l)}} \hat{u}_{2,j}^- + \overline{p_{1,j}^{(l)}} \hat{u}_{1,j}^+ + \overline{p_{2,j}^{(l)}} \hat{u}_{2,j}^+ \right)$$

and second that

$$\int_D \sqrt{|q|} f \cdot \operatorname{curl} \overline{v_j^{(l)-}} \,\mathrm{d}x = 8\pi^2 w_j^* \left(-\overline{p_{1,j}^{(l)}} \hat{u}_{1,j}^- - \overline{p_{2,j}^{(l)}} \hat{u}_{2,j}^- + \overline{p_{1,j}^{(l)}} \hat{u}_{1,j}^+ + \overline{p_{2,j}^{(l)}} \hat{u}_{2,j}^+ \right).$$

This shows that H^* is indeed given by (19). Next we show the compactness of H^*. This relies on the operator $W : \ell^2(\mathbb{Z}^2)^4 \to \ell^2(\mathbb{Z}^2)^4$ defined by

$$W : \begin{pmatrix} a_j^{(1)+} \\ a_j^{(1)-} \\ a_j^{(2)+} \\ a_j^{(2)-} \end{pmatrix}_{j \in \mathbb{Z}^2} \mapsto \left(-8\pi^2 w_j^* \begin{pmatrix} \overline{p_{1,j}^{(1)}} (a_j^{(1)+} + a_j^{(1)-}) + \overline{p_{2,j}^{(1)}} (a_j^{(2)+} + a_j^{(2)-}) \\ \overline{p_{1,j}^{(2)}} (a_j^{(1)+} + a_j^{(1)-}) + \overline{p_{2,j}^{(2)}} (a_j^{(2)+} + a_j^{(2)-}) \\ \overline{p_{1,j}^{(1)}} (a_j^{(1)+} - a_j^{(1)-}) + \overline{p_{2,j}^{(1)}} (a_j^{(2)+} - a_j^{(2)-}) \\ \overline{p_{1,j}^{(2)}} (a_j^{(1)+} - a_j^{(1)-}) + \overline{p_{2,j}^{(2)}} (a_j^{(2)+} - a_j^{(2)-}) \end{pmatrix} \right)_{j \in \mathbb{Z}^2}. \tag{21}$$

Since $(w_j^*)_{j\in\mathbb{Z}^2}$ is a bounded sequence, and since the sequences $(p_j^{(l)})_{j\in\mathbb{Z}^2}$ are bounded for $l=1,2$ due to (15), the operator W is bounded. Now we define the operator

$$Q : L^2(D)^3 \to \ell^2(\mathbb{Z}^2)^4 \tag{22}$$

which maps f to $(\hat{u}_{1,j}^+, \hat{u}_{1,j}^-, \hat{u}_{2,j}^+, \hat{u}_{2,j}^-)^\top$ where u is the radiating variational solution to $\operatorname{curl}^2 u - k^2 u = \operatorname{curl}(\sqrt{|q|}f)$ in Ω. Then we have

$$H^* = -WQ. \tag{23}$$

The following trace spaces are necessary for our proof: Recalling that $e_3 = (0,0,1)^\top$, we define

$$Y(\Gamma_{\pm h}) := \{f \in H^{-1/2}(\Gamma_{\pm h})^3 : \text{ There exists } u \in H_\alpha(\operatorname{curl},\Omega_h) \text{ with } \pm e_3 \times u|_{\Gamma_{\pm h}} = f\}$$

with norm

$$\|f\|_{Y(\Gamma_{\pm h})} = \inf_{u\in H_\alpha(\operatorname{curl},\Omega_h),\, \pm e_3\times u|_{\Gamma_{\pm h}}=f} \|u\|_{H_\alpha(\operatorname{curl},\Omega_h)}.$$

The trace spaces $Y(\Gamma_{\pm h})$ are Banach spaces with this norm, see [30]. In the latter reference it is also shown that the operation $u \mapsto (\pm e_3 \times u|_{\Gamma_{\pm h}}) \times (\pm e_3)$ is bounded from $H_\alpha(\operatorname{curl},\Omega_h)$ into $Y(\Gamma_{\pm h})^*$, the dual space of $Y(\Gamma_{\pm h})$.

Now we know that the operation which maps $f \in L^2(D)^3$ to $u \in H_{\alpha,\mathrm{loc}}(\operatorname{curl},\Omega)$, the radiating variational solution to $\operatorname{curl}^2 u - k^2 u = \operatorname{curl}(\sqrt{|q|}f)$, is bounded. Note that $(\pm e_3 \times u|_{\Gamma_{\pm h}}) \times (\pm e_3) = (u_1, u_2, 0)$. We obtain that the operations $f \mapsto (u_1,u_2,0)|_{\Gamma_h}$ and $(u_1,u_2,0)|_{\Gamma_h} \mapsto (\hat{u}_{1,j}^+, \hat{u}_{2,j}^+)$ are bounded from $L^2(D)^3$ into $Y(\Gamma_h)^*$ and from $Y(\Gamma_h)^*$ into $\ell^2(\mathbb{Z}^2)^2$, respectively. The analogous result holds on Γ_{-h}. Together with the boundedness of the sequence $(w_j^*)_{j\in\mathbb{Z}^2}$ this implies that Q is a bounded operator. Additionally, we know that the field u solves the Helmholtz equation in a neighborhood of $\Gamma_{\pm h}$ since it is divergence-free. Elliptic regularity results [29] imply that u is H^2-regular in a neighborhood of $\Gamma_{\pm h}$. Thus, Rellich's lemma implies that the mapping $f \mapsto (u_1,u_2,0)|_{\Gamma_{\pm h}}$ is compact from $L^2(D)^3$ into $Y(\Gamma_{\pm h})^*$. In consequence, Q is a compact operator and H^* as well as H are compact, too.

To prove the injectivity of H, we show that H^* has dense range. It is sufficient to prove that W has dense range and that all sequences $(\delta_{jl},0,0,0)_{l\in\mathbb{Z}^2}^\top$, $(0,\delta_{jl},0,0)_{l\in\mathbb{Z}^2}^\top$, $(0,0,\delta_{jl},0)_{l\in\mathbb{Z}^2}^\top$ and $(0,0,0,\delta_{jl})_{l\in\mathbb{Z}^2}^\top$ belong to the range of Q (by definition, the Kronecker symbol δ_{jl} equals one for $j=l$ and zero otherwise). The operator W has dense range due to Assumption (8), since

$$\det\begin{pmatrix} \overline{p_{1,j}^{(1)}} & \overline{p_{1,j}^{(1)}} & \overline{p_{2,j}^{(1)}} & \overline{p_{2,j}^{(1)}} \\ \overline{p_{1,j}^{(2)}} & \overline{p_{1,j}^{(2)}} & \overline{p_{2,j}^{(2)}} & \overline{p_{2,j}^{(2)}} \\ \overline{p_{1,j}^{(1)}} & -\overline{p_{1,j}^{(1)}} & \overline{p_{2,j}^{(1)}} & -\overline{p_{2,j}^{(1)}} \\ p_{1,j}^{(2)} & -p_{1,j}^{(2)} & p_{2,j}^{(2)} & -p_{2,j}^{(2)} \end{pmatrix} = -4\left(\overline{p_{1,j}^{(2)}p_{2,j}^{(1)}} - \overline{p_{2,j}^{(2)}p_{1,j}^{(1)}}\right)^2 = \frac{4\overline{\beta_j}^2}{(|\beta_j|^2+\alpha_{2,j}^2)(|\beta_j|^2+\alpha_{1,j}^2)} \neq 0.$$

Finally, we show that $(\delta_{jl},0,0,0)_{l\in\mathbb{Z}^2}^\top$ belongs to the range of Q. (All other cases where the Kronecker symbol appears at a different entry of $0 \in \mathbb{C}^4$ can be treated analogously.) We choose a cut-off function $\chi_1 \in \mathbb{C}^\infty(\mathbb{R})$ such that $\chi_1(t) = 0$ for $t<0$ and $\chi_1(t) = 1$ for $t > h/2$. Then the "upper" Rayleigh sequence of $(x_1,x_2,x_3) \mapsto \chi_1(x_3)\exp(\mathrm{i}(\alpha_j \cdot x + \beta_j(x_3-h)))$ equals $(\delta_{jl})_{l\in\mathbb{Z}^2}$ while the "lower" Rayleigh sequence vanishes. For all $j \in \mathbb{Z}^2$, we define the auxiliary function

$$\chi_{3,j}(x_3) = -\mathrm{i}\alpha_{1,j} e^{-\mathrm{i}\beta_j x_3} \int_0^{x_3} e^{\mathrm{i}\beta_j t}\chi_1(t)\,\mathrm{d}t\,, \quad x_3 \in \mathbb{R}.$$

and set

$$\varphi_j(x) = (\chi_1(x_3), 0, \chi_{3,j}(x_3))^\top \exp(\mathrm{i}(\alpha_j \cdot x + \beta_j(x_3 - h))), \quad x \in \Omega,$$

By construction of φ_j, the Rayleigh sequences of its first two components are $(\delta_{jl}, 0, 0, 0)^\top_{l\in\mathbb{Z}^2}$. Moreover, it holds that $\operatorname{div}\varphi_j = 0$ in Ω. It remains to show that there exists $f_j \in L^2(D)^3$ such that $\operatorname{curl}^2\varphi_j - k^2\varphi_j = \operatorname{curl}(\sqrt{|q|}f_j)$ holds in the variational sense in Ω. Setting

$$g_j(x) := \operatorname{curl}^2\varphi_j(x) - k^2\varphi_j(x), \quad x \in \Omega,$$

we obtain that $\operatorname{div}(g_j) = 0$ in Ω which implies by the divergence theorem that

$$\int_{\partial\Omega_h} g_j \cdot \nu \,\mathrm{d}S = 0.$$

Therefore, due to Theorem 3.38 in [30], there exists $\psi_j \in H^1(\Omega_h)^3$ such that

$$g_j = \operatorname{curl}\psi_j \qquad \text{in } \Omega_h.$$

The function $f_j = \sqrt{|q|}^{-1}\psi_j$ belongs to $L^2(D)^3$ since we supposed in Assumption 1 that $\operatorname{Re}(q) \geq c > 0$. Moreover, it holds in the weak sense that

$$\operatorname{curl}^2\varphi_j - k^2\varphi_j = \operatorname{curl}(\sqrt{|q|}f_j) \quad \text{in } \Omega_h.$$

Note that the above choice of the cut-off function χ implies that ψ_j and g_j are smooth functions for $x_3 > h/2$. Together with the Maxwell's equations $\operatorname{curl}^2\varphi_j - k^2\varphi_j = 0$ that hold in the strong sense in $\Omega \setminus \Omega_{h/2}$, this completes the proof. □

Now we show a factorization of the near-field operator N. To this end, it is convenient to introduce the sign of q, defined by

$$\operatorname{sign}(q) := \frac{q}{|q|} \quad \text{in } \Omega.$$

Theorem 5. *Assume that q satisfies the Assumption 1 and recall the operator W from (21). Define $T : L^2(D)^3 \to L^2(D)^3$ by $Tf = \operatorname{sign}(q)(f + \sqrt{|q|}\operatorname{curl} v)$, where $v \in H_{\alpha,loc}(\operatorname{curl},\Omega)$ is the radiating variational solution to $\operatorname{curl}(\epsilon_r^{-1}\operatorname{curl} v) - k^2 = -\operatorname{curl}(q/\sqrt{|q|}\,f)$ in Ω, see (11). Then the near-field operator satisfies*

$$WN = H^*TH. \tag{24}$$

Proof. We recall the definition of the operator Q in (22), mapping $f \in L^2(D)^3$ to the Rayleigh sequences $(\hat{u}^+_{1,j}, \hat{u}^-_{1,j}, \hat{u}^+_{2,j}, \hat{u}^-_{2,j})^\top_{j\in\mathbb{Z}^2}$ in $\ell^2(\mathbb{Z}^2)^4$, where u is the radiating variational solution to $\operatorname{curl}^2 u - k^2 u = \operatorname{curl}(\sqrt{|q|}f)$ in Ω. By definition of the solution operator G in (12) it holds that

$$Gf = \left(\hat{u}^+_{1,j}, \hat{u}^-_{1,j}, \hat{u}^+_{2,j}, \hat{u}^-_{2,j}\right)^\top_{j\in\mathbb{Z}^2}$$

where $u \in H_{\alpha,\mathrm{loc}}(\operatorname{curl},\Omega)$ is a radiating weak solution to $\operatorname{curl}(\varepsilon_\mathrm{r}^{-1}\operatorname{curl} u) - k^2 u = -\operatorname{curl}(q/\sqrt{|q|}f)$. This means that

$$\operatorname{curl}^2 u - k^2 u = -\operatorname{curl}(\sqrt{|q|}\operatorname{sign}(q)(f + \sqrt{|q|}\operatorname{curl} v)) \quad \text{in } \Omega,$$

thus, $Gf = -(QT)f$. Due to the fact that $N = GH$ this shows that

$$WN = WGH = -WQTH.$$

Additionally we know from (23) that $H^* = -WQ$ which completes the proof. □

4 Analytic Properties of the Middle Operator

Certain analytic properties of the middle operator T from the factorization (24) of Theorem 5 are crucial to establish a Factorization method that characterizes the support D of a biperiodic structure from the corresponding near-field operator N. A crucial property is for instance the coercivity of the selfadjoint part $\operatorname{Re}(T)$ that, essentially, is due to Assumption 1 on the contrast q. All properties that we check in the following lemma are necessary to apply the range identity stated in Theorem 10 in the appendix to the factorization (24) of N. This application and the resulting Factorization method will be discussed in detail in the next Section 5.

Lemma 6. *Suppose that the contrast q satisfies the Assumption 1 and that the direct scattering problem (11) is uniquely solvable for any $f \in L^2(D)^3$. Let $T : L^2(D)^3 \to L^2(D)^3$ be the operator defined in Theorem 5, i.e.*

$$Tf = \operatorname{sign}(q)(f + \sqrt{|q|}\operatorname{curl} v),$$

where $v \in H_{\alpha,loc}(\operatorname{curl},\Omega)$ is the radiating variational solution to

$$\operatorname{curl}(\varepsilon_{\mathrm{r}}^{-1}\operatorname{curl} u) - k^2 u = -\operatorname{curl}(q/\sqrt{|q|}f) \qquad \text{in } \Omega. \tag{25}$$

(a) T is injective and $\langle \operatorname{Im} Tf, f\rangle_{L^2(D)^3} \le 0$ for all $f \in L^2(D)^3$.
(b) Define $T_0 : L^2(D)^3 \to L^2(D)^3$ by $T_0 f = \operatorname{sign}(q)(f + \sqrt{|q|}\operatorname{curl}\tilde{v})$ where $\tilde{v} \in H_{\alpha,\mathrm{loc}}(\operatorname{curl},\Omega)$ solves (25) for $k = \mathrm{i}$ in the variational sense. Then $T - T_0$ is compact on $L^2(D)^3$.
(c) If $\operatorname{Re}(q) > 0$ in D, then there exists $c > 0$ such that $\langle \operatorname{Re}(T_0)f, f\rangle_{L^2(D)^3} \ge c\|f\|^2_{L^2(D)^3}$ for all $f \in L^2(D)^3$, where T_0 is defined in (b).

Note that the proofs of (b) and (c) can be found in [32, Th. 4.9] or in [23, Th. 5.12]. Here, for convenience, we repeat the proof of (b) from [23] with slight adaptations.

Proof. (a) We show the injectivity of T by assuming that $Tf = \operatorname{sign}(q)(f + \sqrt{|q|}\operatorname{curl} v) = 0$ for some $f \in L^2(D)^3$. By definition of T this means that $v \in H_{\alpha,\mathrm{loc}}(\operatorname{curl},\Omega)$ is a radiating variational solution to the homogeneous problem $\operatorname{curl}^2 v - k^2 v = 0$ in Ω. However, we showed in the proof of Lemma 4 that the latter problem has only the trivial solution which implies that $v = 0$ in Ω. Thus, $f = 0$ and T is injective.

To show the semidefiniteness of

$$\langle \operatorname{Im} Tf, f\rangle = \operatorname{Im}\int_D Tf\cdot\overline{f}\,\mathrm{d}x\,, \qquad f \in L^2(D)^3,$$

we set $w = f + \sqrt{|q|}\operatorname{curl} v$. Then $Tf = \operatorname{sign}(q)w$ and

$$\begin{aligned}\langle Tf, f\rangle_{L^2(D)^3} &= \int_D \operatorname{sign}(q)w\cdot(\overline{w} - \sqrt{|q|}\operatorname{curl}\overline{v})\,\mathrm{d}x\\ &= \int_D (\operatorname{sign}(q)|w|^2 - \frac{q}{\sqrt{|q|}}\,w\cdot\operatorname{curl}\overline{v})\,\mathrm{d}x\,.\end{aligned}$$

We consider a smooth cut-off function $\chi \in C^\infty(\mathbb{R})$ such that $\chi(t) = 1$ for $|t| < h$ and $\chi(t) = 0$ for $|t| > 2h$. Then $x \mapsto \chi(x_3)v(x)$ belongs to $H_{\alpha,\mathrm{loc}}(\operatorname{curl},\Omega)$ with compact support in Ω_{3h}. Since

$v \in H_{\alpha,\mathrm{loc}}(\mathrm{curl},\Omega)$ is the radiating solution to (25), it holds that

$$-\int_D \frac{q}{\sqrt{|q|}}\, w\cdot\operatorname{curl}\overline{v}\,\mathrm{d}x = \int_{\Omega_h}(|\operatorname{curl} v|^2 - k^2|v|^2)\,\mathrm{d}x + \int_{\Omega_{2h}\setminus\Omega_h}(\operatorname{curl} v\cdot\operatorname{curl}(\overline{\chi v}) - k^2 v\cdot\overline{\chi v})\,\mathrm{d}x\,.$$

Now using Green's theorems and exploiting that v solves the Helmholtz equation in $\Omega\setminus\Omega_h$, we obtain that

$$\begin{aligned}-\int_D \frac{q}{\sqrt{|q|}}\, w\cdot\operatorname{curl}\overline{v}\,\mathrm{d}x &= \int_{\Omega_h}(|\operatorname{curl} v|^2 - k^2|v|^2)\,\mathrm{d}x + \left(\int_{\Gamma_h} - \int_{\Gamma_{-h}}\right)(e_3\times\operatorname{curl} v\cdot\overline{v})\,\mathrm{d}S\\ &= \int_{\Omega_h}(|\operatorname{curl} v|^2 - k^2|v|^2)\,\mathrm{d}x + \left(\int_{\Gamma_h} - \int_{\Gamma_{-h}}\right)(-\overline{v_1}\partial_3 v_1 - \overline{v_2}\partial_3 v_2 + v_3\partial_3\overline{v_3})\,\mathrm{d}S\,. \qquad (26)\end{aligned}$$

Taking the imaginary part of the latter equation yields

$$-\operatorname{Im}\int_D \frac{q}{\sqrt{|q|}}\, w\cdot\operatorname{curl}\overline{v}\,\mathrm{d}x = \operatorname{Im}\left(\int_{\Gamma_h} - \int_{\Gamma_{-h}}\right)(-\overline{v_1}\partial_3 v_1 - \overline{v_2}\partial_3 v_2 + v_3\partial_3\overline{v_3})\,\mathrm{d}S\,.$$

Recall that v satisfies the radiating Rayleigh condition for $|x_3| > h$. Thus, replacing h in the last equation by $r \geq h$, all the terms corresponding to evanescent modes tend to zero as r tends to infinity, and a straightforward computation shows that

$$\begin{aligned}-\operatorname{Im}\int_D \frac{q}{\sqrt{|q|}}\, w\cdot\operatorname{curl}\overline{v}\,\mathrm{d}x &= \lim_{r\to\infty}\operatorname{Im}\left(\int_{\Gamma_r} - \int_{\Gamma_{-r}}\right)(-\overline{v_1}\partial_3 v_1 - \overline{v_2}\partial_3 v_2 + v_3\partial_3\overline{v_3})\,\mathrm{d}S\\ &= -4\pi^2\sum_{j:k^2>\alpha_j^2}\beta_j(|\hat{v}_j^+|^2 + |\hat{v}_j^-|^2).\end{aligned}$$

Since $\operatorname{Im}(q) \leq 0$ in D, this implies that

$$\begin{aligned}\langle \operatorname{Im} Tf, f\rangle_{L^2(D)^3} &= \int_D \frac{\operatorname{Im}(q)}{\sqrt{|q|}}\,|w|^2\,\mathrm{d}x - \operatorname{Im}\int_D \frac{q}{\sqrt{|q|}}\, w\cdot\operatorname{curl}\overline{v}\,\mathrm{d}x\\ &= \int_D \frac{\operatorname{Im}(q)}{\sqrt{|q|}}\,|w|^2\,\mathrm{d}x - 4\pi^2\sum_{j:k^2>\alpha_j^2}\beta_j(|\hat{v}_j^+|^2 + |\hat{v}_j^-|^2) \leq 0.\end{aligned}$$

(b) From the definitions of T and T_0 we note that $Tf - T_0 f = q/\sqrt{|q|}\operatorname{curl}(v-\tilde{v})$ where $v, \tilde{v} \in H_{\alpha,\mathrm{loc}}(\mathrm{curl},\Omega)$ are the radiating solutions to

$$\int_\Omega (\varepsilon_{\mathrm{r}}^{-1}\operatorname{curl} v\cdot\operatorname{curl}\overline{\psi} - k^2 v\cdot\overline{\psi})\,\mathrm{d}x = -\int_\Omega q/\sqrt{|q|} f\cdot\operatorname{curl}\overline{\psi}\,\mathrm{d}x \quad \text{and} \qquad (27)$$

$$\int_\Omega (\varepsilon_{\mathrm{r}}^{-1}\operatorname{curl}\tilde{v}\cdot\operatorname{curl}\overline{\psi} + \tilde{v}\cdot\overline{\psi})\,\mathrm{d}x = -\int_\Omega q/\sqrt{|q|} f\cdot\operatorname{curl}\overline{\psi}\,\mathrm{d}x\,, \qquad (28)$$

respectively, for all $\psi \in H_\alpha(\mathrm{curl}, \Omega)$ with compact support. By substituting $\psi = \nabla\varphi$ for some $\varphi \in H^1_\alpha(\Omega)$ with compact support we obtain that $\int_\Omega v \cdot \nabla\overline{\varphi}\,\mathrm{d}x = 0$. This means that $\mathrm{div}\, v = 0$ in Ω; analogously, one obtains that $\mathrm{div}\,\tilde{v} = 0$ in Ω. The difference $w = v - \tilde{v}$ hence solves

$$\int_\Omega (\varepsilon_\mathrm{r}^{-1}\,\mathrm{curl}\, w \cdot \mathrm{curl}\,\overline{\psi} - k^2 w \cdot \overline{\psi})\,\mathrm{d}x = (k^2+1)\int_\Omega \tilde{v}\cdot\overline{\psi}\,\mathrm{d}x\,,$$

for all $\psi \in H_\alpha(\mathrm{curl}, \Omega)$ with compact support.

To prove the compactness of $T - T_0$, we choose a sequence f_j that converges weakly to zero in $L^2(D)^3$ and denote by $v_j, \tilde{v}_j \in H_{\alpha,\mathrm{loc}}(\mathrm{curl}, \Omega)$ the corresponding radiating and bounded solutions to (27) and (28), respectively. If we set $w_j := v_j - \tilde{v}_j \in H_{\alpha,\mathrm{loc}}(\mathrm{curl}, \Omega)$, then it remains to show that

$$(T - T_0) f_j = \frac{q}{\sqrt{|q|}}\,\mathrm{curl}(v_j - \tilde{v}) = \frac{q}{\sqrt{|q|}}\,\mathrm{curl}(w_j)$$

tends to zero strongly in $L^2(D)^3$.

By the boundedness of the solution operator mapping f_j to v_j and $\tilde{v}_j$, we conclude that w_j converges weakly to zero in $H_\alpha(\mathrm{curl}, \Omega_h)$. Furthermore, v_j and $\tilde{v}_j$ are smooth outside of $\overline{D}$ and hence converge strongly to zero in $H^s(\Gamma_{\pm h})^3$ for all $s \geq 0$. Using standard Sobolev embedding results we find that $w_j = v_j - \tilde{v}_j$ converges to zero in the maximum norm on $\Gamma_{\pm h}$. Let us next define the subspace

$$H^1_{\alpha,\diamond}(\Omega_h) = \left\{ \varphi \in H^1_\alpha(\Omega_h) : \int_{\Omega_h} \varphi\,\mathrm{d}S = 0 \right\}$$

of $H^1_\alpha(\Omega_h)$ and determine $p_j \in H^1_{\alpha,\diamond}(\Omega_h)$ as the solution to

$$\int_{\Omega_h} \nabla p_j \cdot \nabla\overline{\varphi}\,\mathrm{d}x = \left(\int_{\Gamma_h} + \int_{\Gamma_{-h}}\right)(\nu \cdot w_j)\overline{\varphi}\,\mathrm{d}S \qquad \text{for all } \varphi \in H^1_{\alpha,\diamond}(\Omega_h). \tag{29}$$

The solution of (29) exists and is unique since the form $(p,\varphi) \mapsto \int_{\Omega_h} \nabla p \cdot \nabla\varphi\,\mathrm{d}x$ is bounded and coercive on $H^1_{\alpha,\diamond}(\Omega_h)$ by the inequality of Poincaré [16]: There exists a constant $c > 0$ with

$$\int_{\Omega_h} |\nabla\varphi|^2\,\mathrm{d}x \geq c\|\varphi\|^2_{H^1_\alpha(\Omega_h)} \qquad \text{for all } \varphi \in H^1_{\alpha,\diamond}(\Omega_h). \tag{30}$$

Problem (29) is the variational form of the Neumann boundary value problem $\Delta p_j = 0$ in Ω_h, $\partial p_j/\partial\nu = \nu \cdot w_j$ on $\partial\Omega_h$. We observe that (29) holds even for all $\varphi \in H^1_\alpha(\Omega_h)$ since $\int_{\partial\Omega_h}(\nu \cdot w_j)\,\mathrm{d}S$ vanishes by the divergence theorem and since $\mathrm{div}\, w_j = 0$. Substituting $\varphi = p_j$ into (29) yields, by exploiting (30) and the trace theorem,

$$\begin{aligned} c\|p_j\|^2_{H^1_\alpha(\Omega_h)} \leq \int_{\Omega_h} |\nabla p_j|^2\,\mathrm{d}x &= \left(\int_{\Gamma_h} + \int_{\Gamma_{-h}}\right)(\nu \cdot w_j)\overline{p_j}\,\mathrm{d}S \\ &\leq C\left(\|w_j\|_{C(\Gamma_h)^3} + \|w_j\|_{C(\Gamma_{-h})^3}\right)\|p_j\|_{H^1_\alpha(\Omega_h)}. \end{aligned}$$

Consequently, the convergence $\|w_j\|_{C(\Gamma_{\pm h})^3} \to 0$ as $j \to \infty$ that we found above implies that $\|p_j\|_{H^1_\alpha(\Omega_h)}$ tends to zero, too.

If we subtract ∇p_j from w_j, then the resulting function $\tilde{w}_j := w_j - \nabla p_j \in H_\alpha(\mathrm{curl}, \Omega_h)$ even belongs to the closed subspace

$$H_{\alpha,\mathrm{div}\,0}(\mathrm{curl}, \Omega_h) := \left\{ u \in H_\alpha(\mathrm{curl}, \Omega_h) : \int_{\Omega_h} \nabla\varphi \cdot u \,\mathrm{d}x = 0 \text{ for all } \varphi \in H^1_\alpha(\Omega_h) \right\}$$

of $H_\alpha(\mathrm{curl}, \Omega_h)$. This subspace is well-known to be compactly embedded in $L^2(\Omega_h)^3$, see [35], or [30, Theorem 4.7]. Additionally, we have already shown above that w_j tends to zero weakly in $H_\alpha(\mathrm{curl}, \Omega_h)$ as $j \to \infty$. Since $\nabla p_j \to 0$ strongly in $L^2(\Omega_h)^3$, we conclude by the compact embedding of $H_{\alpha,\mathrm{div}\,0}(\mathrm{curl}, \Omega_h)$ in $L^2(\Omega_h)^3$ that $\tilde{w}_j \to 0$ strongly in $L^2(\Omega_h)^3$. Hence, $w_j \to 0$ strongly in $L^2(\Omega_h)^3$, too.

Now we return to the variational equation for w_j and substitute $\psi = \phi\overline{w_j}$ where $\phi \in C^\infty(\mathbb{R}^3)$ is some α-quasiperiodic function with compact support such that $\phi = 1$ on Ω_h. This yields

$$\begin{aligned}\int_{\Omega_h} (\varepsilon_\mathrm{r}^{-1} |\operatorname{curl} w_j|^2 - k^2 |w_j|^2) \,\mathrm{d}x \;&= \int_{\Omega\setminus\Omega_h} (\varepsilon_\mathrm{r}^{-1} \operatorname{curl} w_j \cdot \operatorname{curl}(\phi\overline{w_j}) - k^2 \phi |w_j|^2) \,\mathrm{d}x \\ &\quad + (k^2+1) \int_\Omega \phi \tilde{v}_j \cdot \overline{w_j} \,\mathrm{d}x\,.\end{aligned}$$

Note that the function w_j is smooth in $\Omega \setminus \Omega_h$ and that ϕ has compact support. This allows to integrate by parts in $\Omega \setminus \Omega_h$, and to exploit the equation $\operatorname{curl}^2 w_j - k^2 w_j = (k^2+1)\tilde{v}_j$ to get that

$$\int_{\Omega_h} (\varepsilon_\mathrm{r}^{-1} |\operatorname{curl} w_j|^2 - k^2 |w_j|^2) \,\mathrm{d}x \;= \left(\int_{\Gamma_h} + \int_{\Gamma_{-h}} \right) (\nu \times \operatorname{curl} w_j) \cdot \overline{w_j} \,\mathrm{d}S \;+ (k^2+1) \int_{\Omega_h} \tilde{v}_j \cdot \overline{w_j} \,\mathrm{d}x\,.$$

The right-hand side in the last equation tends to zero as $j \to \infty$ since, first, $\|w_j\|_{C(\Gamma_{\pm h})^3} \to 0$ as $j \to \infty$ and since $\|\operatorname{curl} w_j\|_{L^2(\Gamma_{\pm h})^3} \le C$ for all $j \in \mathbb{N}$. Second, we showed above that $\|w_j\|_{L^2(\Omega_h)^3}$ tends to zero and that $\|\tilde{v}_j\|_{L^2(\Omega_h)^3}$ is bounded as $j \to \infty$. Therefore, $\operatorname{curl} w_j$ tends to zeros in $L^2(\Omega_h)^3$, which completes the proof. □

5 Characterization of the Biperiodic Structure

In this section, we use the near-field operator N, or equivalently, certain Rayleigh coefficients of scattered electromagnetic waves, to characterize explicitly when a point z belongs to the support of the contrast q. This characterization exploits special test sequences that we construct from the Rayleigh sequences of an α-quasiperiodic Green's tensor. The principle ingredients for proving this characterization are the factorization of the near-field operator, the properties of the operators involved in this factorization, and the range identity of Theorem 10. We also deduce a simple and fast algorithm for imaging the periodic structure, which is known as the Factorization method.

First we introduce some basic facts about α-quasiperiodic Green's functions. It is well-known that the function

$$G_k(x,y) = \frac{\mathrm{i}}{8\pi^2} \sum_{j\in\mathbb{Z}} \frac{1}{\beta_j} e^{\mathrm{i}\alpha_j\cdot(x-y)+\mathrm{i}\beta_j|x_3-y_3|}, \quad x, y \in \Omega,\ x_3 \neq y_3, \tag{31}$$

is the scalar radiating α-quasiperiodic Green's function of the Helmholtz operator in three dimensions. This means that, for fixed $y \in \Omega$,

$$\Delta_x G_k(x,y) + k^2 G_k(x,y) = -\delta_y(x)$$

holds in the distributional sense in Ω. The difference of G_k and the radiating fundamental solution of the Helmholtz equation in free-space is smooth, see, e.g. [2],

$$G_k(x,y) = \frac{e^{\mathrm{i}k|x-y|}}{4\pi|x-y|} + \Psi_k(x-y), \quad x,y \in \Omega,\ x_3 \neq y_3, \tag{32}$$

where Ψ_k is an analytic solution to the Helmholtz equation in $(-2\pi, 2\pi)^2 \times \mathbb{R}$.

The α-quasiperiodic Green's tensor $\mathbb{G}_k(x,y) \in \mathbb{C}^{3\times 3}$ defined by

$$\mathbb{G}_k(x,y) = G_k(x,y)\mathrm{I}_{3\times 3} + k^{-2}\nabla_x \mathrm{div}_x(G_k(x,y)\mathrm{I}_{3\times 3}), \quad x,y \in \Omega,\ x_3 \neq y_3,$$

solves, for fixed $y \in \Omega$,

$$\mathrm{curl}_x^2\, \mathbb{G}_k(x,y) - k^2 \mathbb{G}_k(x,y) = \delta_y(x)\mathrm{I}_{3\times 3}$$

in the distributional sense in Ω, where $\mathrm{I}_{3\times 3}$ denotes the identity matrix in $\mathbb{C}^{3\times 3}$. Here, the curl of a matrix is taken columnwise, and the div of a matrix and the ∇ are meant to be taken columnwise and componentwise, respectively. Note that $\mathbb{G}_k$ satisfies the Rayleigh expansion condition and has a strong singularity due to the representation of G_k in (32).

Lemma 7. *Recall the operators H^* and W from (19) and (21), respectively, and the support $\overline{D}$ of the contrast q from Assumption 1. For any $z \in \Omega$ and fixed nonzero $p = (p_1, p_2, p_3)^\top \in \mathbb{C}^3$ we denote by $(\hat{\Psi}_{z,j})_{j\in\mathbb{Z}^2} \in \ell^2(\mathbb{Z}^2)^4$ the upper and lower Rayleigh coefficients of the first two components of*

$$\begin{aligned}\Psi_z(x) &:= k^2 \mathbb{G}_k(x,z)p \\ &= \begin{pmatrix} \left[k^2 G_k(x,z) + \frac{\partial^2 G_k(x,z)}{\partial x_1^2}\right]p_1 + \frac{\partial^2 G_k(x,z)}{\partial x_1 \partial x_2}p_2 + \frac{\partial^2 G_k(x,z)}{\partial x_1 \partial x_3}p_3 \\ \frac{\partial^2 G_k(x,z)}{\partial x_2 \partial x_1}p_1 + \left[k^2 G_k(x,z) + \frac{\partial^2 G_k(x,z)}{\partial x_2^2}\right]p_2 + \frac{\partial^2 G_k(x,z)}{\partial x_2 \partial x_3}p_3 \\ \frac{\partial^2 G_k(x,z)}{\partial x_3 \partial x_1}p_1 + \frac{\partial^2 G_k(x,z)}{\partial x_3 \partial x_2}p_2 + \left[k^2 G_k(x,z) + \frac{\partial^2 G_k(x,z)}{\partial x_3^2}\right]p_3 \end{pmatrix}, \quad x \in \Omega,\ x_3 \neq z_3.\end{aligned} \tag{33}$$

Then z belongs to D if and only if $W(\hat{\Psi}_{j,z}) \in \mathrm{Rg}(H^*)$.

Remark 8. *The upper and lower Rayleigh sequences $(\hat{G}^{\pm}_{k,j}(z))_{j\in\mathbb{Z}^2}$ of the α-quasiperiodic Green's function $G_k(\cdot, z)$ can be obtained from the representation (31),*

$$\hat{G}^{\pm}_{k,j}(z) = \frac{\mathrm{i}}{8\pi^2\beta_j} e^{-\mathrm{i}[\alpha_{1,j}z_1 + \alpha_{2,j}z_2 \pm \beta_j(z_3 \mp h)]}, \qquad j \in \mathbb{Z}^2.$$

Thus, the Rayleigh sequences $(\hat{\Psi}_{z,j})_{j\in\mathbb{Z}^2} \in \ell^2(\mathbb{Z}^2)^4$ of the first two components of Ψ_z can be computed analogously. Explicitly, the upper and lower Rayleigh coefficients, denoted by $(\hat{\Psi}^+_{z,j})_{j\in\mathbb{Z}^2}$ and by $(\hat{\Psi}^-_{z,j})_{j\in\mathbb{Z}^2} \in \ell^2(\mathbb{Z}^2)^2$, respectively, are

$$\hat{\Psi}^{\pm}_{z,j} = \begin{pmatrix} (k^2 - \alpha_{1,j}^2)\hat{G}^{\pm}_{k,j}(z)p_1 - \alpha_{1,j}\alpha_{2,j}\hat{G}^{\pm}_{k,j}(z)p_2 \mp \alpha_{1,j}\beta_j \hat{G}^{\pm}_{k,j}(z)p_3 \\ -\alpha_{2,j}\alpha_{1,j}\hat{G}^{\pm}_{k,j}(z)p_1 + (k^2 - \alpha_{2,j}^2)\hat{G}^{\pm}_{k,j}(z)p_2 \mp \alpha_{2,j}\beta_j \hat{G}^{\pm}_{k,j}(z)p_3 \end{pmatrix}, \quad j \in \mathbb{Z}^2.$$

Proof. First, let $z \in D$ belong to the interior of the support of the contrast q. Recall the operator Q defined in (22). Due to $H^* = -WQ$ it is sufficient to show that $(\hat{\Psi}_{z,j})_{j\in\mathbb{Z}^2} \in \mathrm{Rg}(Q)$. Choose $r > 0$ such that $B(z,r) \in D$ and consider a cut-off function $\varphi \in C^\infty(\mathbb{R}^3)$ with $\varphi(x) = 0$ for $|x - z| \le r/2$ and $\varphi(x) = 1$ for $|x - z| \ge r$. We define

$$w(x) = \operatorname{curl}^2(\varphi(x)\mathbb{G}_k(x,z)p), \quad x \in \Omega,$$

and note that w is a smooth, quasiperiodic function in $H_\alpha(\operatorname{curl},\Omega)$ due to (32). Note that

$$w(x) = \operatorname{curl}^2(\varphi(x)\mathbb{G}_k(x,z)p) = k^2\mathbb{G}_k(x,z)p \qquad \text{for } |x-z| \ge r,$$

and further that all Rayleigh sequences of w and of Ψ_z are equal. Using Green's theorem we obtain

$$\begin{aligned}\int_\Omega (\operatorname{curl} w \cdot \operatorname{curl}\overline{\psi} - k^2 w\cdot\overline{\psi})\,\mathrm{d}x &= \int_\Omega (\operatorname{curl} w - k^2 \operatorname{curl}(\varphi(x)\mathbb{G}_k(x,z)p))\cdot\operatorname{curl}\overline{\psi}\,\mathrm{d}x\\ &= \int_\Omega g\cdot\operatorname{curl}\overline{\psi}\,\mathrm{d}x\,,\end{aligned}$$

for all $\psi \in H_\alpha(\operatorname{curl},\Omega)$ with compact support, and $g := \operatorname{curl} w - k^2\operatorname{curl}(\varphi(x)\mathbb{G}_k(x,z)p)$. Since $x \mapsto g(x)$ is smooth and vanishes for $|z - x| \ge r$, it holds that $\operatorname{supp}(g) \subset D$. Setting $f := \sqrt{|q|}^{-1} g \in L^2(D)^3$, we obtain that

$$\int_\Omega (\operatorname{curl} w \cdot \operatorname{curl}\overline{\psi} - k^2 w\cdot\overline{\psi})\,\mathrm{d}x = \int_D \sqrt{|q|} f\cdot\operatorname{curl}\overline{\psi}\,\mathrm{d}x$$

for all $\psi \in H_\alpha(\operatorname{curl},\Omega)$ with compact support. This implies that $(\hat{\Psi}_{z,j})_{j\in\mathbb{Z}^2} \in \mathrm{Rg}(Q)$.

Now let $z \notin D$, and assume, on the contrary, that $\hat{\Psi}_{z,j} \in \mathrm{Rg}(Q)$. This means that there exists $u \in H_{\alpha,\mathrm{loc}}(\operatorname{curl},\Omega)$ and $f \in L^2(D)^3$ such that u is the variational radiating solution to $\operatorname{curl}^2 u - k^2 u = \operatorname{curl}(\sqrt{|q|}f)$ and, additionally, that the tangential components of the upper and lower Rayleigh sequences of u and of Ψ_z are equal. Since the first two components of the Rayleigh sequences are equal, the tangential components of the two functions must be equal. Both functions are divergence-free in $(0,2\pi)^2 \times \{|x_3| > h\}$, which implies that $u = \Psi_z$ in $(0,2\pi)^2 \times \{|x_3| > h\}$. Due to the analyticity of u and Ψ_z in $\Omega \setminus D$ and in $\Omega \setminus \{z\}$, respectively, we conclude by analytic continuation that $u = \Psi_z$ in $\Omega \setminus (D \cup \{z\})$. This is a contradiction since $u \in H(\operatorname{curl}, B)$ for any ball $B \subset \Omega$ containing z but $\operatorname{curl}(k^2\mathbb{G}_k(\cdot,z)p) \notin H(\operatorname{curl}, B)$ due to the strongly singularity of $\mathbb{G}_k(\cdot,z)$ at z. □

Our main theorem on the Factorization method for biperiodic electromagnetic inverse scattering is now a simple corollary of the previous chapters combined with the range identity from Theorem 10.

Theorem 9 (Main Theorem – Factorization Method)**.** *Suppose that the contrast q and the domain D satisfy Assumption 1 and that the direct scattering problem* (11) *is uniquely solvable. Denote by $\big(\lambda_n, (\phi_{n,j})_{j\in\mathbb{Z}^2}\big)_{n\in\mathbb{N}}$ the orthonormal eigensystem of $(WN)_\sharp = |\mathrm{Re}\,(WN)| + \mathrm{Im}\,(WN)$ and by $(\hat{\Psi}_{z,j})_{j\in\mathbb{Z}^2}$ the test sequence from Lemma 7. Then a point $z \in \Omega$ belongs to the domain D if and only if*

$$\sum_{n=1}^{\infty} \frac{|\langle (\hat{\Psi}_{z,j})_{j\in\mathbb{Z}^2},\ (\phi_{n,j})_{j\in\mathbb{Z}^2}\rangle_{\ell^2(\mathbb{Z}^2)^4}|^2}{\lambda_n} < \infty. \tag{34}$$

Proof. As we assumed in the theorem, $\big(\lambda_n,\,(\phi_{n,j})_{j\in\mathbb{Z}^2}\big)_{n\in\mathbb{N}}$ is an orthonormal eigensystem of the selfadjoint operator $(WN)_\sharp : \ell^2(\mathbb{Z}^2)^4 \to \ell^2(\mathbb{Z}^2)^4$. The assumptions of Theorem 10 on H, H^* and T in the factorization $WN = H^*TH$ from Lemma 5 have been checked in Lemmas 4 and 6 (strictly speaking, the assumptions on the middle operator have been checked for $-T$). Therefore, an application of Theorem 10 yields that $\mathrm{Rg}((WN)_\sharp^{1/2}) = \mathrm{Rg}(H^*)$. Combining this range identity with the characterization given in Lemma 7, we obtain that $(\hat\Psi_{z,j}^\pm)_{j\in\mathbb{Z}^2} \in \mathrm{Rg}((WN)_\sharp^{1/2})$ if and only if $z \in D$. The criterion (34) follows now directly from Picard's range criterion; the terms in the series in (34) are well-defined since $\lambda_n > 0$ due to Theorem 10. □

6 Numerical Experiments

As mentioned in the introduction, we present in this section a couple of numerical experiments for imaging of biperiodic obstacles via the Picard criterion (34). To the best of our knowledge, these are the first three-dimensional numerical examples for the Factorization method in a biperiodic electromagnetic setting. Our numerical examples focus on the dependence of the computed images on the number of incident fields, on the number of evanescent modes needed for a "reasonable" reconstruction, and on the performance of the method when the synthetically computed data are perturbed by artificial noise.

The synthetic near-field data required for inversion experiments have been obtained from numerical solutions to the direct scattering problem. We computed these solutions using an extension of a volume integral equation method for the scalar H-mode case studied in [27] to the Maxwell's equations. This extension yields a numerical method that is shown to converge quasi-optimally in $H_\alpha(\mathrm{curl},\Omega_h)$, as it is shown in the thesis [31]. For $M_1, M_2 \in \mathbb{N}$, we introduce

$$\mathbb{Z}^2_{M_1,M_2} := \{j = (j_1,j_2)^\top \in \mathbb{Z}^2 : -M_1 \le j_1, j_2 \le M_2\}.$$

For the numerical experiments presented below we solve the direct problem for a number of incident fields $\varphi_j^{(l)\pm}$ where $j \in \mathbb{Z}^2_{M_1,M_2}$, and compute the Rayleigh coefficients of the scattered fields, again for all indices in $\mathbb{Z}^2_{M_1,M_2}$. Denote by $\boldsymbol{N}_{M_1,M_2}$ the block matrix of the corresponding discretization of the near-field operator N,

$$\boldsymbol{N}_{M_1,M_2} = \begin{pmatrix} \left((\hat u_{1,n}^+)_j^{(1)+}\right)_{j,n} & \left((\hat u_{1,n}^+)_j^{(1)-}\right)_{j,n} & \left((\hat u_{1,n}^+)_j^{(2)+}\right)_{j,n} & \left((\hat u_{1,n}^+)_j^{(2)-}\right)_{j,n} \\ \left((\hat u_{2,n}^+)_j^{(1)+}\right)_{j,n} & \left((\hat u_{2,n}^+)_j^{(1)-}\right)_{j,n} & \left((\hat u_{2,n}^+)_j^{(2)+}\right)_{j,n} & \left((\hat u_{2,n}^+)_j^{(2)-}\right)_{j,n} \\ \left((\hat u_{1,n}^-)_j^{(1)+}\right)_{j,n} & \left((\hat u_{1,n}^-)_j^{(1)-}\right)_{j,n} & \left((\hat u_{1,n}^-)_j^{(2)+}\right)_{j,n} & \left((\hat u_{1,n}^-)_j^{(2)-}\right)_{j,n} \\ \left((\hat u_{2,n}^-)_j^{(1)+}\right)_{j,n} & \left((\hat u_{2,n}^-)_j^{(1)-}\right)_{j,n} & \left((\hat u_{2,n}^-)_j^{(2)+}\right)_{j,n} & \left((\hat u_{2,n}^-)_j^{(2)-}\right)_{j,n} \end{pmatrix}, \tag{35}$$

where the indices j, n in each subblock belong both to $\mathbb{Z}^2_{M_1,M_2}$. Here, $\hat u^\pm_{(1,2),n}$ are the two tangential components of the Rayleigh coefficients of the scattered defined field defined in (13). Moreover, for $l = 1, 2$, the notation $(\,\cdot\,)_j^{(l)\pm}$ indicates the dependence of these Rayleigh coefficients on the corresponding incident field $\varphi_j^{(l)\pm}$.

Each of the 16 sub-matrices of $\boldsymbol{N}_{M_1,M_2}$ is a matrix of size $(M_1+M_2+1)^2 \times (M_1+M_2+1)^2$. Thus, $\boldsymbol{N}_{M_1,M_2}$ is a matrix of size $4(M_1+M_2+1)^2 \times 4(M_1+M_2+1)^2$. The matrix $\boldsymbol{W}\boldsymbol{N}_{M_1,M_2}$,

which corresponds to the discretization of the operator product WN from, e.g., Theorem 9, can be computed directly using (19). The hermitean matrix $\mathrm{Re}\,(\boldsymbol{W}\boldsymbol{N}_{M_1,M_2})$, where the selfadjoint part is again defined as in (1), possesses an eigendecomposition

$$\mathrm{Re}\,(\boldsymbol{W}\boldsymbol{N}_{M_1,M_2}) = \boldsymbol{V}\boldsymbol{D}\boldsymbol{V}^{-1},$$

where $\boldsymbol{D}$ is the diagonal matrix containing the eigenvalues of $\mathrm{Re}\,(\boldsymbol{W}\boldsymbol{N}_{M_1,M_2})$ and $\boldsymbol{V}$ is the orthogonal matrix of the corresponding eigenvectors. Denote by $|\boldsymbol{D}|$ the absolute value of $\boldsymbol{D}$ which is taken elementwise. Then

$$(\boldsymbol{W}\boldsymbol{N}_{M_1,M_2})_\sharp := \boldsymbol{V}\,|\boldsymbol{D}|\,\boldsymbol{V}^{-1} + \mathrm{Im}\,(\boldsymbol{W}\boldsymbol{N}_{M_1,M_2}).$$

We compute another eigenvalue decomposition of $(\boldsymbol{W}\boldsymbol{N}_{M_1,M_2})_\sharp = \boldsymbol{\Phi}\boldsymbol{\Lambda}\boldsymbol{\Phi}^{-1}$ with a diagonal matrix $\boldsymbol{\Lambda}$ that contains the $4(M_1+M_2+1)^2$ eigenvalues $\boldsymbol{\lambda}_n$ of $(\boldsymbol{W}\boldsymbol{N}_{M_1,M_2})_\sharp$ and an orthogonal matrix $\boldsymbol{\Phi} = (\boldsymbol{\phi}_{j,n})_{j,n=1}^{4(M_1+M_2+1)^2}$ containing the eigenvectors $(\boldsymbol{\phi}_{j,n})_{j=1}^{4(M_1+M_2+1)^2}$. Then

$$(\boldsymbol{W}\boldsymbol{N}_{M_1,M_2})_\sharp^{1/2} = \boldsymbol{\Phi}\,|\boldsymbol{\Lambda}|^{1/2}\,\boldsymbol{\Phi}^{-1}. \tag{36}$$

The test sequences $(\hat{\Psi}_{z,j})_{j\in\mathbb{Z}^2} \in \ell^2(\mathbb{Z}^2)^4$ have to be discretized according to the discretization of the near-field operator, and we denote this discretization by $(\hat{\boldsymbol{\Psi}}_{z,j})_{j=1}^{4(M_1+M_2+1)^2}$. Then the criterion (34) is numerically exploited for imaging by plotting the function

$$z \mapsto P_{M_1,M_2}(z) := \left[\sum_{n=1}^{4(M_1+M_2+1)^2} \frac{|A_n(z)|^2}{\boldsymbol{\lambda}_n}\right]^{-1} \qquad \text{where } A_n(z) = \sum_{j=1}^{4(M_1+M_2+1)^2} \hat{\boldsymbol{\Psi}}_{z,j}\overline{\boldsymbol{\phi}_{j,n}}. \tag{37}$$

If the series in (37) approximates the true value of the exact Picard series in (34), then P_{M_1,M_2} should be very small outside of D and considerably larger inside D.

To show the performance of the method with noisy data, we perturb our synthetic data by artificial noise. More precisely, we add a complex-valued noise matrix $\boldsymbol{X}$ containing random numbers that are uniformly distributed in the complex square $\{a+\mathrm{i}b,\, |a|\le 1,\, |b|\le 1\} \subset \mathbb{C}$ to the data matrix $(\boldsymbol{W}\boldsymbol{N}_{M_1,M_2})_\sharp^{1/2}$. Denoting by δ the noise level, the noisy data matrix $(\boldsymbol{W}\boldsymbol{N}_{M_1,M_2})_{\sharp,\delta}^{1/2}$ is then given by

$$(\boldsymbol{W}\boldsymbol{N}_{M_1,M_2})_{\sharp,\delta}^{1/2} := (\boldsymbol{W}\boldsymbol{N}_{M_1,M_2})_\sharp^{1/2} + \delta\frac{\boldsymbol{X}}{\|\boldsymbol{X}\|_2}\left\|(\boldsymbol{W}\boldsymbol{N}_{M_1,M_2})_\sharp^{1/2}\right\|_2,$$

where $\|\cdot\|_2$ is the matrix 2-norm. Note that the latter equation implies that

$$\frac{\left\|(\boldsymbol{W}\boldsymbol{N}_{M_1,M_2})_{\sharp,\delta}^{1/2} - (\boldsymbol{W}\boldsymbol{N}_{M_1,M_2})_\sharp^{1/2}\right\|_2}{\left\|(\boldsymbol{W}\boldsymbol{N}_{M_1,M_2})_\sharp^{1/2}\right\|_2} = \delta. \tag{38}$$

Obviously, for such noisy discrete data, the eigenvalue decomposition in (36) has to be replaced by a singular value decomposition, that we will not detail here. Following the traditional way

of implementing sampling methods, we apply Tikhonov regularization [13], that is, instead of implementing (37) we consider

$$z \mapsto P_{N_1,M_2,\delta}(z) := \left[\sum_{n=1}^{4(M_1+M_2+1)^2} \frac{\boldsymbol{\lambda}_n^\delta}{\left(\boldsymbol{\lambda}_n^\delta + \gamma\right)^2} |A_n^\delta(z)|^2 \right]^{-1} \tag{39}$$

where $\boldsymbol{\lambda}_n^\delta$ are the singular values of the perturbed data matrix $(\boldsymbol{W}\boldsymbol{N}_{M_1,M_2})_{\sharp,\delta}^{1/2}$ and $A_n^\delta(z)$ is the corresponding perturbation of the function A_n from (37) (that has now to be defined using the left singular vectors of the perturbed data matrix). The parameter γ is chosen according to Morozov's discrepancy principle by approximately solving the non-linear scalar equation

$$\sum_{n=1}^{4(M_1+M_2+1)^2} \frac{\gamma^2 - \delta^2 \boldsymbol{\lambda}_n^\delta}{(\boldsymbol{\lambda}_n^\delta + \gamma)^2} |A_n^\delta(z)|^2 = 0 \qquad \text{for } \gamma = \gamma(\delta, z)$$

at each sampling point z.

All the following experiments rely on three different biperiodic structures that are defined in one period $\Omega = (-\pi, \pi)^2 \times \mathbb{R}$ in terms of the support $\overline{D}$ of the contrast q as follows:

(i) A biperiodic structure of ellipsoids with constant contrast,

$$\begin{aligned} \overline{D} &= \{x = (x_1, x_2, x_3)^\top \in \Omega : \frac{x_1^2}{2.5^2} + \frac{x_2^2}{2.5^2} + \frac{x_3^2}{0.4^2} \leq 1\}, \\ q(x) &= 0.5 \quad \text{in } D. \end{aligned} \tag{40}$$

(ii) A biperiodic structure of cubes with variable contrast that is smooth within D,

$$\begin{aligned} \overline{D} &= \{x = (x_1, x_2, x_3)^\top \in \Omega : |x_1| \leq 2.5, |x_2| \leq 2.5, |x_3| \leq 0.45\}, \\ q(x) &= (x_3 + 1)(\sin(x_1)^2 \sin(x_2)^2 + 0.3)/4 - 0.4\mathrm{i} \quad \text{in } D. \end{aligned} \tag{41}$$

(iii) A plate with biperiodically aligned rectangular holes with piecewise constant contrast,

$$\begin{aligned} \overline{D} &= \left\{ x = (x_1, x_2, x_3)^\top \in \Omega : \, |x_3| \leq 0.45 \text{ and } \left(|x_1| \leq 1.75 \text{ or } |x_2| \leq 1.75\right) \right\}, \\ q(x) &= \begin{cases} 0.5 - 0.6\mathrm{i} & \text{in } D_1 = \{(x_1, x_2)^\top \in D : -1 < x_1 < 1\}, \\ 0.3 & \text{in } D \setminus D_1. \end{cases} \end{aligned} \tag{42}$$

The wave number k is the same for all experiments and equals $2\pi/3$. Further, we note that all reconstructions have been smoothed using the command `smooth3` in Matlab. Even if we merely reconstruct one period of the structure, we plot 3×3 periods of the obtained images to better illustrate the periodicity. The isovalue for plotting the images is chosen by hand such that the size of the reconstruction roughly remains the same for all examples. At this point, a-priori knowledge about the size of the volume of the structure is, at least implicitly, used.

Figure 1 shows that the imaging method crucially depends on a sufficient number of accurate near-field measurements. Definitely, if one only measures the propagating modes of the scattered field, then the resulting images of the biperiodically aligned ellipsoids are not useful.

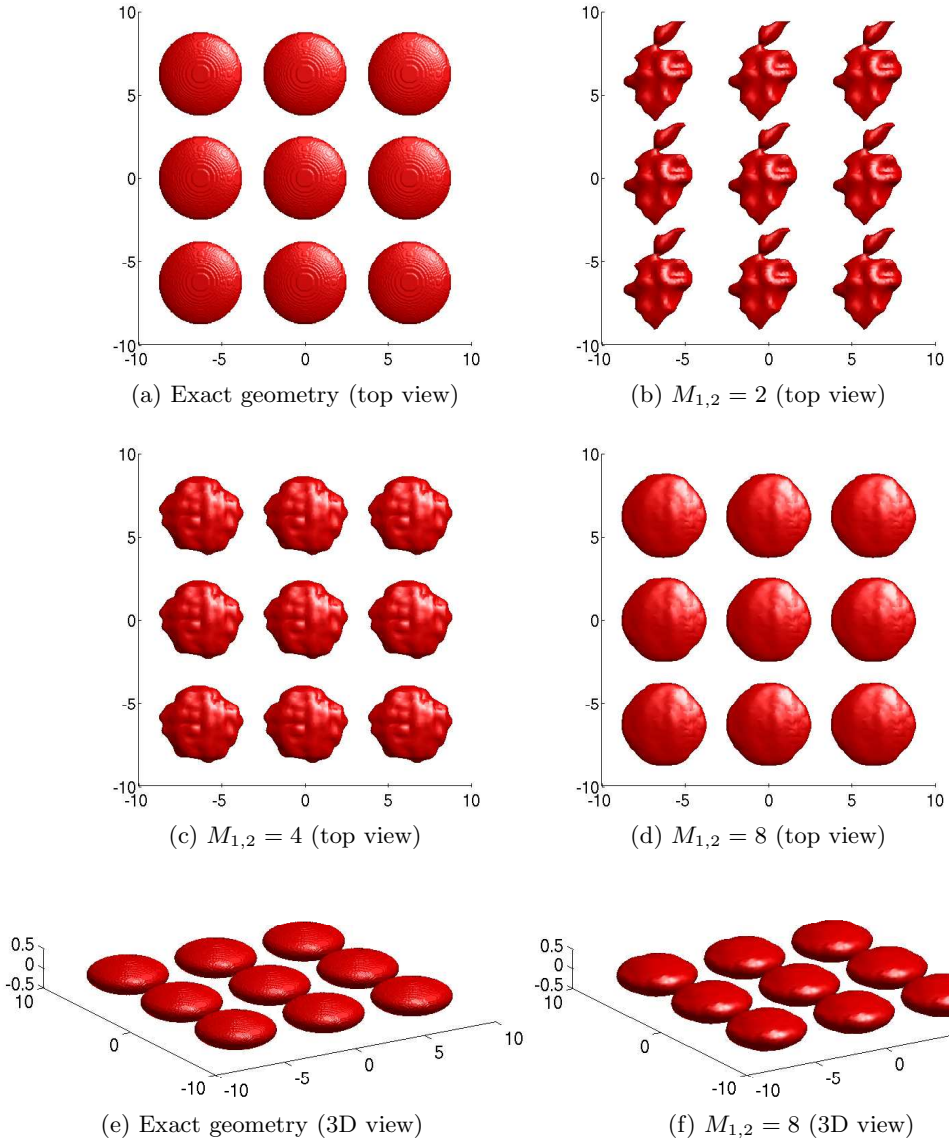

(a) Exact geometry (top view)

(b) $M_{1,2} = 2$ (top view)

(c) $M_{1,2} = 4$ (top view)

(d) $M_{1,2} = 8$ (top view)

(e) Exact geometry (3D view)

(f) $M_{1,2} = 8$ (3D view)

Figure 1: Reconstructions of ellipsoids for different numbers of incident fields. The number of Rayleigh coefficients used for the images is $4(M_1 + M_2 + 1)^2$, cf. the image captions. No artificial noise has been added to the data. (a) Exact geometry (see (40)) (b) 48 propagating modes, 52 evanescent modes, isovalue 7 (c) 52 propagating modes, 312 evanescent modes, isovalue 0.1 (d) 52 propagating modes, 1104 evanescent modes, isovalue 0.01.

Figure 2 shows that the same imaging experiment for biperiodically aligned cubes defined in (41). Despite the contrast is now varying within D, the conclusion from the first experiment remains essentially the same. Since the corresponding experiment for the third structure, the biperiodically aligned crosses from (42) shows essentially the same behavior, we do not show the resulting images.

Figures 3 and 4 show the dependence of the images for the periodically aligned ellipsoids and

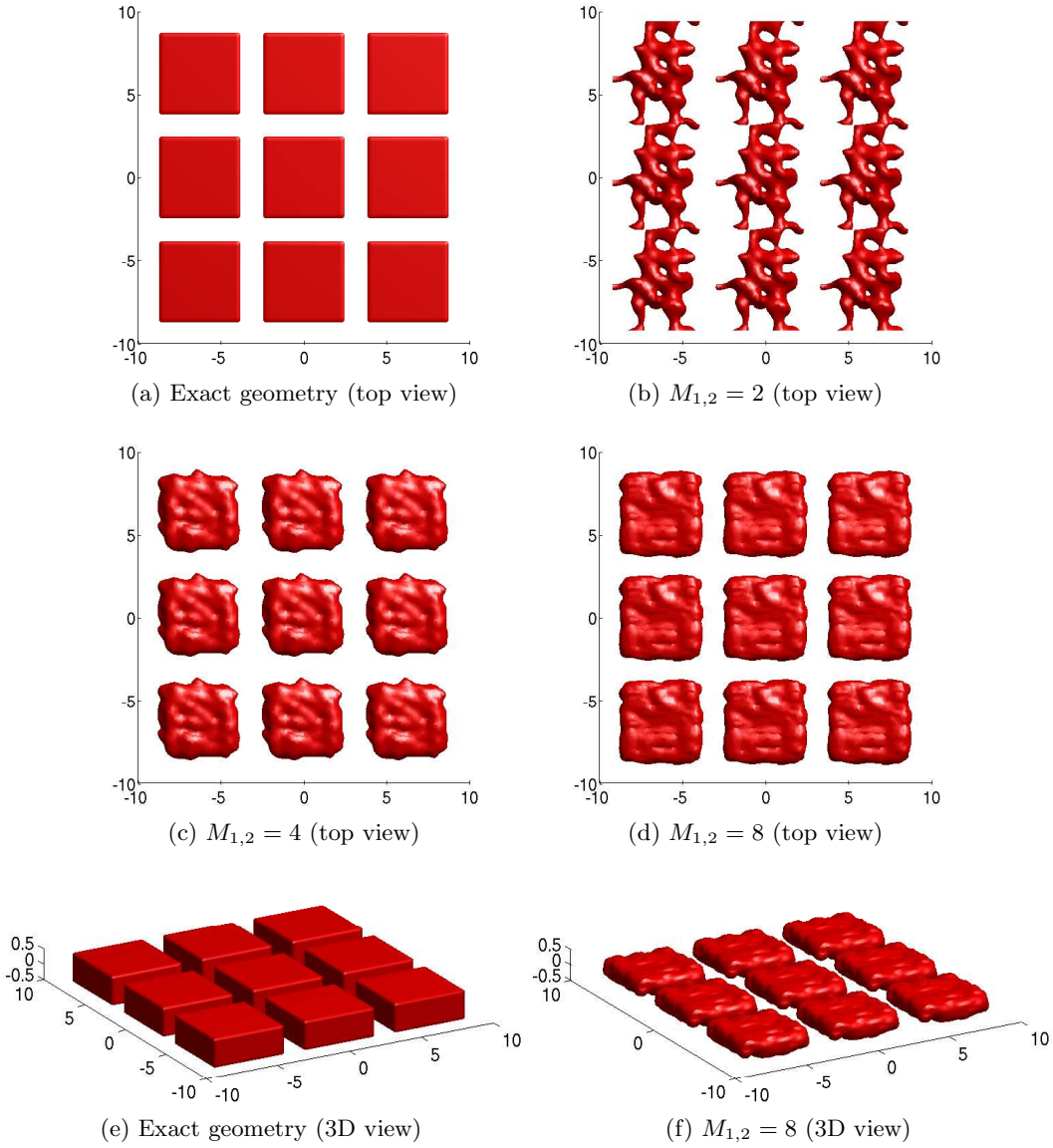

(a) Exact geometry (top view) (b) $M_{1,2} = 2$ (top view)

(c) $M_{1,2} = 4$ (top view) (d) $M_{1,2} = 8$ (top view)

(e) Exact geometry (3D view) (f) $M_{1,2} = 8$ (3D view)

Figure 2: Reconstructions of cubes for different numbers of incident fields. The number of Rayleigh coefficients used for the images is $4(M_1 + M_2 + 1)^2$, cf. the image captions. No artificial noise has been added to the data. (a) Exact geometry (see (41)) (b) 48 propagating modes, 52 evanescent modes, isovalue 40 (c) 52 propagating modes, 312 evanescent modes, isovalue 1.8 (d) 52 propagating modes, 1104 evanescent modes, isovalue 0.008.

cubes from the last two figures on the artificial noise level. The noise is added as described above and the noise level is measured in the matrix 2-norm, see (38). We consider noise levels of 2 and 5 percent, that is, $\delta = 0.02$ and $\delta = 0.05$. Figure 5 shows the same numerical experiment for the periodically aligned crosses that we defined in (42). All three experiments show that the images computed from data with both 2 and with 5 percent noise level still provide reasonable information on the biperiodic structure. Admittedly, this stability is partly due to the three dimensional setting,

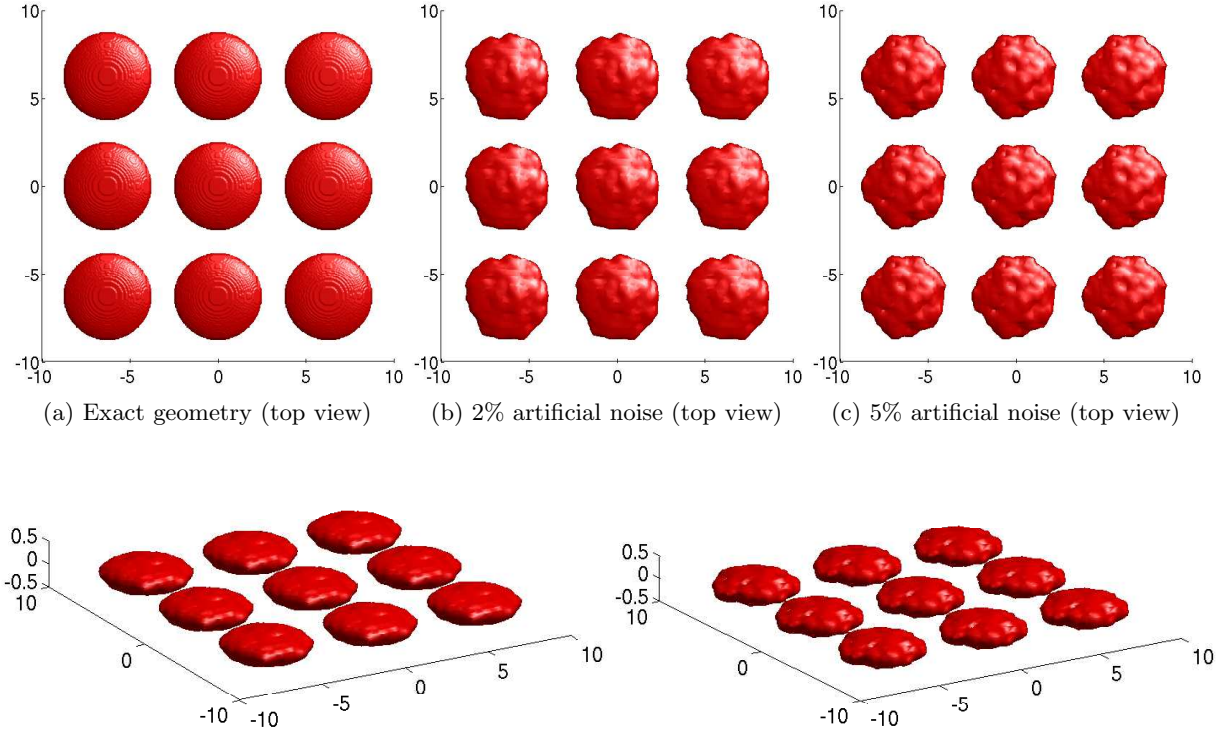

(a) Exact geometry (top view) (b) 2% artificial noise (top view) (c) 5% artificial noise (top view)

(d) 2% artificial noise (3D view) (e) 5% artificial noise (3D view)

Figure 3: Reconstructions of biperiodically aligned ellipsoids with artificial noise on the data. All reconstructions use 52 propagating modes and 1104 evanescent modes ($M_{1,2} = 8$). (a) Exact geometry (see (40) and Figure 1(a),(e)) (b) 2% artificial noise, isovalue 0.0012 (c) 5% artificial noise, isovalue 0.0023 (d) 2% artificial noise, isovalue 0.0012 (e) 5% artificial noise, isovalue 0.0023.

and due the relatively high dimension of the measurement operator.

A The Range Identity Theorem

This appendix presents an abstract result on range identities which is necessary to characterize the support D of the contrast q. Earlier versions of this result can be found in [23, 25]. Since the version presented here is only a slight extension of the earlier versions, we do not give a proof here, but refer to [31] for a complete proof.

To state the result, we introduce real and imaginary part of a bounded linear operator. Let $X \subset U \subset X^*$ be a Gelfand triple, that is, U is a Hilbert space, X is a reflexive Banach space with dual X^* for the inner product of U, and the embeddings are injective and dense. Then the real and imaginary part of a bounded operator $T : X^* \to X$ are defined in accordance with the corresponding definition for complex numbers,

$$\mathrm{Re}\,(T) := \frac{1}{2}(T + T^*), \qquad \mathrm{Im}\,(T) := \frac{1}{2i}(T - T^*).$$

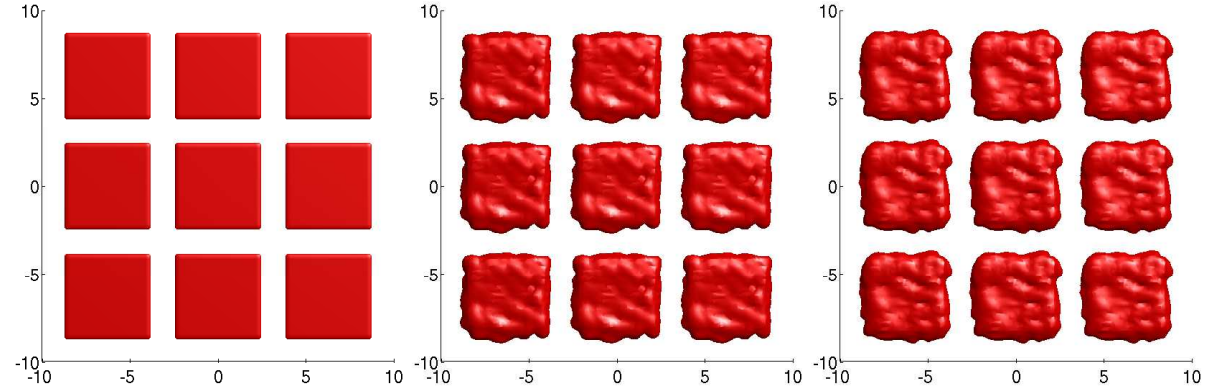

(a) Exact geometry (top view) (b) 2% artificial noise (top view) (c) 5% artificial noise (top view)

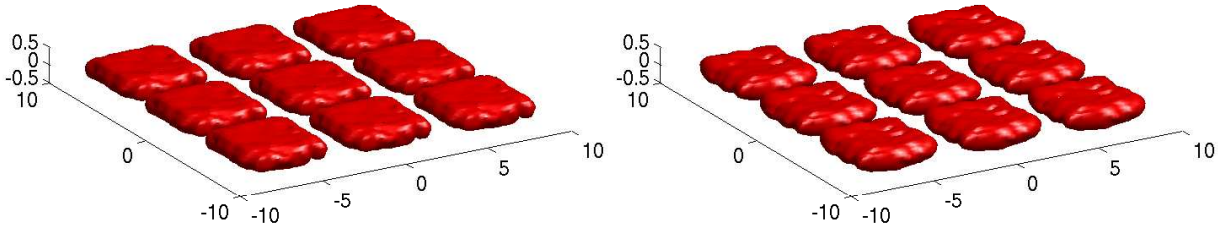

(d) 2% artificial noise (3D view) (e) 5% artificial noise (3D view)

Figure 4: Reconstructions of biperiodically aligned cubes with artificial noise on the data. All reconstructions use 52 propagating modes and 1104 evanescent modes ($M_{1,2} = 8$). (a) Exact geometry (see (41) and Figure 2(a),(e)) (b) 2% artificial noise, isovalue 0.012 (c) 5% artificial noise, isovalue 0.02 (d) 2% artificial noise, isovalue 0.012 (e) 5% artificial noise, isovalue 0.02.

Theorem 10. *Let $X \subset U \subset X^*$ be a Gelfand triple with Hilbert space U and reflexive Banach space X. Furthermore, let V be a second Hilbert space and $F : V \to V$, $H : V \to X$ and $T : X \to X^*$ be linear and bounded operators with*

$$F = H^* T H$$

We make the following assumptions:

a) H is compact and injective.

b) There exists $t \in [0, 2\pi]$ such that $\operatorname{Re}(e^{\mathrm{i}t}T)$ has the form $\operatorname{Re}(e^{\mathrm{i}t}T) = T_0 + T_1$ with some positive definite selfadjoint operator T_0 and some compact operator $T_1 : X \to X^*$.

c) $\operatorname{Im} T$ is non positive on X, i.e., $\langle \operatorname{Im} T\phi, \phi \rangle \leq 0$ for all $\phi \in X$.

Moreover, we assume that one of the two following conditions is fulfilled:

d) T is injective and t from b) does not equal $\pi/2$ or $3\pi/2$.

e) $\operatorname{Im} T$ is negative on the (finite dimensional) null space of $\operatorname{Re}(e^{\mathrm{i}t}T)$, i.e., for all $\phi \neq 0$ such that $\operatorname{Re}(e^{\mathrm{i}t}T)\phi = 0$ it holds $\langle \operatorname{Im} T\phi, \phi \rangle < 0$.

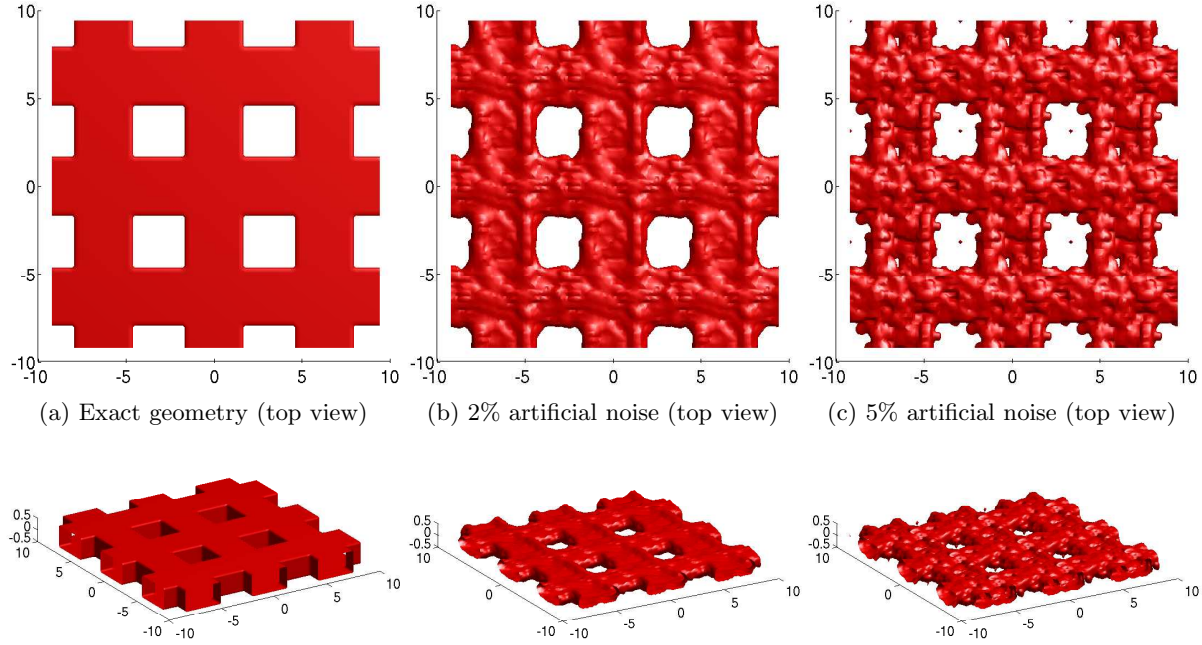

(a) Exact geometry (top view) (b) 2% artificial noise (top view) (c) 5% artificial noise (top view)

(d) Exact geometry (3D view) (e) 2% artificial noise (3D view) (f) 5% artificial noise (3D view)

Figure 5: Reconstructions of biperiodically aligned crosses with artificial noise on the data. All reconstructions use 52 propagating modes and 1104 evanescent modes ($M_{1,2} = 8$). (a) Exact geometry (see (42)) (b) 2% artificial noise, isovalue 0.02 (c) 5% artificial noise, isovalue 0.004 (d) Exact geometry (e) 2% artificial noise, isovalue 0.02 (f) 5% artificial noise, isovalue 0.004.

Then the operator $F_\sharp := |\mathrm{Re}\,(e^{\mathrm{i}t}F)| - \mathrm{Im}\,F$ *is positive definite and the ranges of* $H^* : X^* \to V$ *and* $F_\sharp^{\frac{1}{2}} : V \to V$ *coincide.*

References

[1] H. Ammari, *Uniqueness theorems for an inverse problem in a doubly periodic structures*, Inverse Problems, 11 (1995), pp. 823–833.

[2] T. Arens, *Scattering by biperiodic layered media: The integral equation approach.* Habilitation Thesis, Universität Karlsruhe, 2010.

[3] T. Arens, *Why linear sampling works*, Inverse Problems, 20 (2004), pp. 163–173.

[4] T. Arens and N. Grinberg, *A complete factorization method for scattering by periodic structures*, Computing, 75 (2005), pp. 111–132.

[5] T. Arens and A. Kirsch, *The factorization method in inverse scattering from periodic structures*, Inverse Problems, 19 (2003), pp. 1195–1211.

[6] T. Arens and A. Lechleiter, *The linear sampling method revisited*, J. Int. Eq. Appl., 21 (2009), pp. 179–202.

[7] G. Bao, *Variational approximation of Maxwell's equations in biperiodic structures*, SIAM J. Appl. Math., 57 (1997), pp. 364–381.

[8] G. Bao, H. Zhang, and J. Zou, *Unique determination of periodic polyhedral structures scattered electromagnetic fields*, Trans. Amer. Math. Soc, 9 (2011), pp. 4527–4551.

[9] G. Bao and Z. Zhou, *An inverse problem for scattering by a doubly periodic structure*, Trans. Amer. Math. Soc, 350 (1998), pp. 4089–4103.

[10] F. Cakoni and D. Colton, *Qualitative Methods in Inverse Scattering Theory. An Introduction.*, Springer, Berlin, 2006.

[11] F. Cakoni, D. Colton, and P. Monk, *The Linear Sampling Method in Inverse Electromagnetic Scattering*, SIAM, 2011.

[12] P. S. Carney and J. C. Schotland, *Near-field tomography*, in Inside out: inverse problems and applications, vol. 47 of Math. Sci. Res. Inst. Publ., Cambridge Univ. Press, Cambridge, 2003, pp. 133–168.

[13] D. Colton, J. Coyle, and P. Monk, *Recent developments in inverse acoustic scattering theory*, SIAM Review, 42 (2000), pp. 396–414.

[14] D. Colton and A. Kirsch, *A simple method for solving inverse scattering problems in the resonance region*, Inverse Problems, 12 (1996), pp. 383–393.

[15] D. C. Dobson, *A variational method for electromagnetic diffraction in biperiodic structures*, Math. Model. Numer. Anal., 28 (1994), pp. 419–439.

[16] L. Evans, *Partial Differential Equations*, American Mathematical Society, 1998.

[17] M. Frigo and S. Johnson, *The design and implementation of fftw3*, Proceedings of the IEEE, 93 (2005), pp. 216 –231.

[18] G. Hu, F. Qu, and B. Zhang, *A linear sampling method for inverse problems of diffraction gratings of mixed types*, Math. Meth. Appl. Sci., 35 (2012), pp. 1047–1066.

[19] G. Hu and B. Zhang, *The linear sampling method for the inverse electromagnetic scattering by a partially coated bi-periodic structure*, Math. Meth. Appl. Sci., 34 (2011), pp. 509–519.

[20] C. T. Kelley, *Iterative Methods for Linear and Nonlinear Equations*, Frontiers in Applied Mathematics (No. 16), SIAM, 1995.

[21] A. Kirsch, *Uniqueness theorems in inverse scattering theory for periodic structures*, Inverse Problems, 10 (1994), pp. 145–152.

[22] ——, *Characterization of the shape of a scattering obstacle using the spectral data of the far field operator*, Inverse Problems, 14 (1998), pp. 1489–1512.

[23] A. Kirsch and N. Grinberg, *The Factorization Method for Inverse Problems*, Oxford Lecture Series in Mathematics and its Applications 36, Oxford University Press, 2008.

[24] A. Kirsch and S. Ritter, *A linear sampling method for inverse scattering from an open arc*, Inverse Problems, 16 (2000), pp. 89–105.

[25] A. Lechleiter, *The Factorization method is independent of transmission eigenvalues*, Inverse Problems and Imaging, 3 (2009), pp. 123–138.

[26] ——, *Imaging of periodic dielectrics*, BIT, 50 (2010), pp. 59–83.

[27] A. Lechleiter and D.-L. Nguyen, *A galerkin method for strongly singular volume integral equations arising in grating scattering*, Submitted, (2012).

[28] ——, *Volume integral equations for scattering from anisotropic diffraction gratings*, Mathematical Methods in the Applied Sciences, (2012).

[29] W. McLean, *Strongly Elliptic Systems and Boundary Integral Operators*, Cambridge University Press, Cambridge, UK, 2000.

[30] P. Monk, *Finite Element Methods for Maxwell's Equations*, Oxford Science Publications, Oxford, 2003.

[31] D. L. Nguyen, *Spectral Methods for Direct and Inverse Scattering from Periodic Structures*, PhD thesis, Ecole Polytechnique, Palaiseau, France, 2012.

[32] K. Sandfort, *The factorization method for inverse scattering from periodic inhomogeneous media*, PhD thesis, Karlsruher Institut für Technologie, 2010.

[33] J. Saranen, *On an inequality of Friedrichs'*, Math. Scand., 51 (1982), pp. 310–322.

[34] G. Schmidt, *On the diffraction by biperiodic anisotropic structures*, Appl. Anal., 82 (2003), pp. 75–92.

[35] C. Weber, *A local compactness theorem for Maxwell's equations*, Math. Methods Appl. Sci., 2 (1980), pp. 12–25.

[36] J. Yang and B. Zhang, *A inverse transmission scattering problem for periodic media*, Inverse Problems, 27 (2011), p. 22pp.

[37] J. Yang, B. Zhang, and R. Zhang, *A sampling method for the inverse transmission problem for periodic media*, Inverse Problems, 28 (2012), p. 17pp.